Optics
2026; 14(1): 1-21
http://www.sciencepublishinggroup.com/j/optics
doi: 10.11648/j.optics.20261401.11

Non-classical Features in a Pump-free Hybrid Atom-optomechanical System

Adagn Addisu Dabulo*

Department of Physics, Hawassa University, Hawassa, Ethiopia

Email address:

adagnaddisu@gmail.com (Adagn Addisu Dabulo), adagna@hu.edu.et (Adagn Addisu Dabulo)

To cite this article:

Adagn Addisu Dabulo. (2026). Non-classical Features in a Pump-free Hybrid Atom-optomechanical System. *Optics, 14*(1), 1-21. https://doi.org/10.11648/j.optics.20261401.11

Received: 20 March 2026 ; **Accepted:** 2 April 2026 ; **Published:** 26 May 2026

Abstract: This work investigates the emergence of Non-classical Features in a pump-free hybrid atom-optomechanical system, addressing key limitations of conventional platforms that rely on strong coherent driving and are highly vulnerable to thermal decoherence. We propose a novel architecture in which a squeezed vacuum reservoir acts as a pre-correlated quantum environment, enabling the deterministic generation and stabilization of nonclassical correlations without the need for an external laser pump. By exploiting reservoir-engineered interactions, the system supports robust quadrature squeezing and multipartite entanglement across a wide range of operational parameters. Our analysis demonstrates that the hybrid system achieves significant squeezing levels approaching 90%, while simultaneously satisfying the DGCZ inseparability criterion, confirming the presence of strong continuous-variable entanglement. Importantly, these nonclassical signatures remain resilient under extreme thermal conditions, withstanding thermal occupancies as high as ($n_{\text{th}} = 1500$), which substantially exceeds the tolerance of traditional laser-driven optomechanical systems. The underlying mechanism is attributed to passive correlation injection from the engineered reservoir, which effectively suppresses thermal noise and enhances quantum coherence even in weak-coupling and low-power regimes. This eliminates the need for active pumping, thereby reducing energy consumption and experimental complexity. Furthermore, the hybrid atom-optomechanical configuration introduces additional tunability through atomic gain and population inversion, thereby allowing flexible control over system dynamics and correlation properties. Overall, the proposed scheme establishes a scalable and energy-efficient pathway toward realizing robust quantum correlations in realistic noisy environments. It opens new prospects for cryogen-free quantum technologies, including quantum-enhanced sensing, precision metrology, and long-distance entanglement distribution.

Keywords: Population Inversion, Continuous-variable Entanglement (DGCZ Criterion), Nonclassical Light Generation, Reservoir Squeezing, Optomechanical Cooperativity

1. Introduction

Quantum fluctuations, arising from operator non-commutativity and the intrinsic structure of vacuum fields, constitute a foundational pillar of quantum mechanics. Within cavity optomechanics, such fluctuations manifest as radiation-pressure noise and quantum backaction, phenomena that can be harnessed to realize cooling and entanglement. Hybrid quantum platforms further refine control over these fluctuations[1, 2], particularly in multimode architectures where enhanced mode coupling enables richer dynamical behavior [2–4]. Notably, pump-free protocols employing squeezed vacuum reservoirs have emerged as powerful mechanisms for stabilizing stationary entanglement while circumventing classical noise sources [5, 9]. The generation of robust light-matter entanglement remains indispensable for scalable quantum technologies. In this context, engineered dissipation-through squeezed reservoirs and non-Hermitian dynamics-provides an effective strategy for mitigating decoherence and preserving quantum correlations. [7, 10, 24]

Here, a cascade-type (Ξ-type) atom embedded in a bimodal cavity and coupled to a correlated squeezed bath establishes a versatile platform for multipartite entanglement generation. By tailoring vacuum fluctuations, cavity losses

can be compensated, thereby sustaining squeezing even within strongly dissipative regimes [11]–[27]. Whereas the good-cavity limit ($2g \gg \kappa, \gamma$) promotes coherent energy exchange, the bad-cavity regime ($\kappa \gg \gamma$) facilitates efficient noise suppression. Correlated reservoirs provide a conceptual and operational bridge between these regimes, reinforcing coherence even under substantial damping. When integrated with hybrid CQED and giant-atom architectures, this framework offers a viable pathway toward resilient quantum networks operating in inherently lossy environments [28]–[25]. The hybrid optomechanical system consists of a cascade (Ξ-type) three-level atom interacting simultaneously with bimodal cavity fields, mechanical oscillators, and both squeezed vacuum and thermal reservoirs, treated under the rotating-wave and Born-Markov approximations. These interactions collectively describe atom-reservoir, atom-cavity, cavity-reservoir, cavity-mechanical, and mechanical-thermal bath couplings, thereby forming a unified framework for analyzing dissipative quantum dynamics and multipartite correlations. In the interaction picture, the total Hamiltonian can be decomposed into free and interaction parts as

$$\hat{H}_{\text{total}} = \hat{H}_0 + \hat{H}_{\text{int}}. \tag{1}$$

The free Hamiltonian describing the uncoupled cavity modes, mechanical oscillators, and atomic energy levels is given by

$$\hat{H}_0 = \hbar \sum_{i=1}^{2} \omega_{c_i}\, \hat{a}_i^{\dagger}\hat{a}_i + \hbar \sum_{i=1}^{2} \omega_{m_i}\, \hat{b}_i^{\dagger}\hat{b}_i + \sum_{i=1}^{3} E_i\, \hat{\sigma}_{ii}. \tag{2}$$

The total interaction Hamiltonian incorporating atom-cavity, optomechanical, mechanical-thermal bath, atom-reservoir, and cavity-reservoir couplings is expressed as

$$\begin{aligned}\hat{H}_{\text{int}} = {} & i\hbar \sum_{\substack{i=1 \\ j=i+1}}^{2} g_{a_i}\left(\hat{a}_i\hat{\sigma}_{ji} - \hat{a}_i^{\dagger}\hat{\sigma}_{ij}\right) - \hbar \sum_{i=1}^{2} g_{0_i}\hat{a}_i^{\dagger}\hat{a}_i\left(\hat{b}_i + \hat{b}_i^{\dagger}\right) + \sum_{j=1}^{2}\sum_{k} \hbar g_{k,j}\left(\hat{b}_j\hat{c}_{k,j}^{\dagger} + \hat{b}_j^{\dagger}\hat{c}_{k,j}\right) \\ & + i\hbar \sum_{\substack{i=1 \\ j=i+1}}^{2} \lambda_{ij}\left(\hat{\sigma}_{ji}\hat{c}_{i,\text{in}} - \hat{\sigma}_{ij}\hat{c}_{i,\text{in}}^{\dagger}\right) + i\hbar \sum_{i=1}^{2} \lambda_{cr}\left(\hat{a}_i^{\dagger}\hat{c}_{i,\text{in}} - \hat{a}_i\hat{c}_{i,\text{in}}^{\dagger}\right).\end{aligned} \tag{3}$$

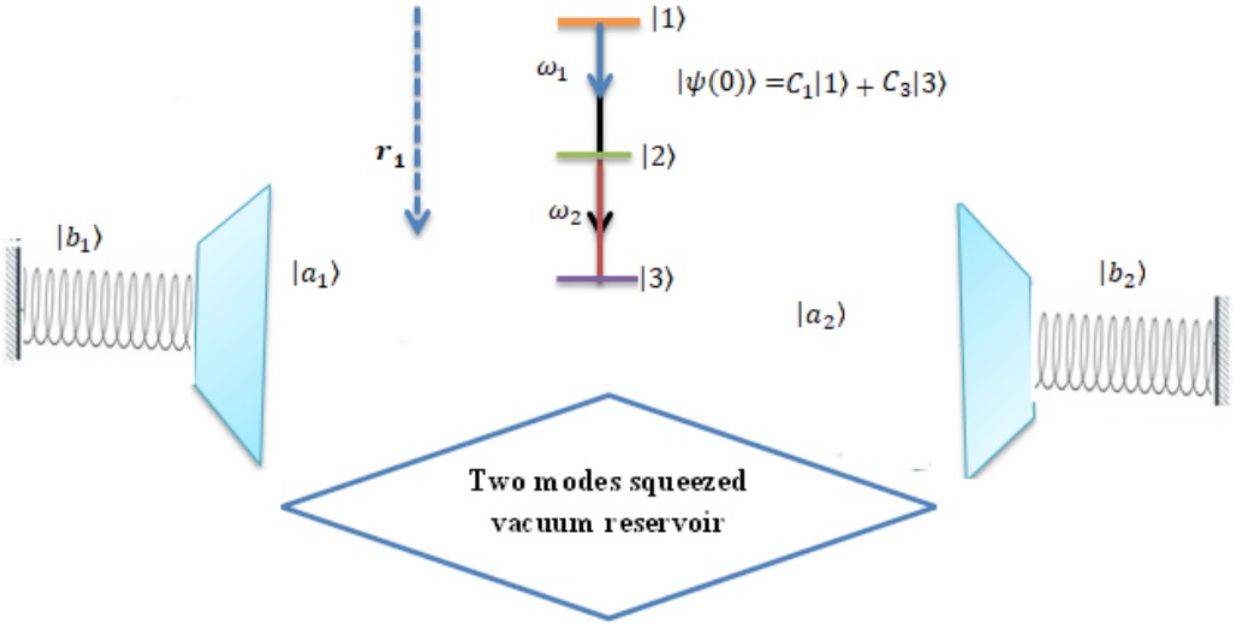

Figure 1. *Schematic representation of Cascade Ξ-type three-level atom interaction with optomechanical cavity coupled to two-mode squeezed vacuum reservoir in bad cavity.*

2. Master Equation

To simplify the dynamics of the hybrid system, we perform an adiabatic elimination of the atomic degrees of freedom. This approach is rigorously justified under the bad-cavity limit $\kappa \gg \gamma$, which establishes the necessary time-scale separation to slave the fast atomic variables to the slower cavity and mechanical modes. Our derivation maintains perturbative consistency by retaining terms to the second order in the coupling strength. Furthermore, the final effective Master Equation is presented in the Lindblad form, thereby preserving the complete positivity of the dynamics and ensuring that all particle populations remain positive-definite. The master equation of the system taking into account for quantum optomechanical system where three level atom interact with vacuum reservoir as:

$$\begin{aligned}\frac{d\hat{\rho}}{dt} &= g\left(\hat{\sigma}_{12}\hat{a}_1\hat{\rho} - \hat{a}_1^\dagger\hat{\sigma}_{21}\hat{\rho} + \hat{\sigma}_{23}\hat{a}_2\hat{\rho} - \hat{a}_2^\dagger\hat{\sigma}_{32}\hat{\rho} - \hat{\rho}\hat{\sigma}_{12}\hat{a}_1 + \hat{\rho}\hat{a}_1^\dagger\hat{\sigma}_{21} - \hat{\rho}\hat{\sigma}_{23}\hat{a}_2 + \hat{\rho}\hat{a}_2^\dagger\hat{\sigma}_{32}\right)\\ &+ iX_1\left(\hat{a}_1^\dagger\hat{a}_1\hat{\rho} - \hat{\rho}\hat{a}_1^\dagger\hat{a}_1\right) + iX_2\left(\hat{a}_2^\dagger\hat{a}_2\hat{\rho} - \hat{\rho}\hat{a}_2^\dagger\hat{a}_2\right)\\ &+ \frac{1}{2}\kappa(N+1)\left(2\hat{a}_1\rho\hat{a}_1^\dagger - \hat{a}_1^\dagger\hat{a}_1\rho - \rho\hat{a}_1^\dagger\hat{a}_1\right) + \frac{1}{2}\kappa N\left(2\hat{a}_1^\dagger\rho\hat{a}_1 - \hat{a}_1\hat{a}_1^\dagger\rho - \rho\hat{a}_1\hat{a}_1^\dagger\right)\\ &+ \frac{1}{2}\kappa(N+1)\left(2\hat{a}_2\rho\hat{a}_2^\dagger - \hat{a}_2^\dagger\hat{a}_2\rho - \rho\hat{a}_2^\dagger\hat{a}_2\right) + \frac{1}{2}\kappa N\left(2\hat{a}_2^\dagger\rho\hat{a}_2 - \hat{a}_2\hat{a}_2^\dagger\rho - \rho\hat{a}_2\hat{a}_2^\dagger\right)\\ &- \kappa M_a\left(\hat{a}_1^\dagger\hat{\rho}\hat{a}_2^\dagger + \hat{a}_2^\dagger\hat{\rho}\hat{a}_1^\dagger - \hat{a}_1^\dagger\hat{a}_2^\dagger\hat{\rho} - \hat{\rho}\hat{a}_1^\dagger\hat{a}_2^\dagger + \hat{a}_1\hat{\rho}\hat{a}_2 + \hat{a}_2\hat{\rho}\hat{a}_1 - \hat{a}_1\hat{a}_2\hat{\rho} - \hat{\rho}\hat{a}_1\hat{a}_2\right)\\ &+ \frac{1}{2}\gamma\left(2\hat{\sigma}_{21}\hat{\rho}\hat{\sigma}_{12} - \hat{\sigma}_{11}\hat{\rho} - \hat{\rho}\hat{\sigma}_{11} + 2\hat{\sigma}_{32}\hat{\rho}\hat{\sigma}_{23} - \hat{\sigma}_{22}\hat{\rho} - \hat{\rho}\hat{\sigma}_{22}\right)\\ &+ \frac{1}{2}\gamma_{m1}(n_{th,1}+1)\left(2\hat{b}_1\hat{\rho}\hat{b}_1^\dagger - \hat{b}_1^\dagger\hat{b}_1\hat{\rho} - \hat{\rho}\hat{b}_1^\dagger\hat{b}_1\right) + \frac{1}{2}\gamma_{m1}n_{th,1}\left(2\hat{b}_1^\dagger\hat{\rho}\hat{b}_1 - \hat{b}_1\hat{b}_1^\dagger\hat{\rho} - \hat{\rho}\hat{b}_1\hat{b}_1^\dagger\right)\\ &+ \frac{1}{2}\gamma_{m2}(n_{th,2}+1)\left(2\hat{b}_2\hat{\rho}\hat{b}_2^\dagger - \hat{b}_2^\dagger\hat{b}_2\hat{\rho} - \hat{\rho}\hat{b}_2^\dagger\hat{b}_2\right) + \frac{1}{2}\gamma_{m2}n_{th,2}\left(2\hat{b}_2^\dagger\hat{\rho}\hat{b}_2 - \hat{b}_2\hat{b}_2^\dagger\hat{\rho} - \hat{\rho}\hat{b}_2\hat{b}_2^\dagger\right). \end{aligned} \tag{4}$$

2.1. The Heisenberg Equation of Motion

In quantum mechanics, operators carry the time dependence in the Heisenberg picture for the cavity and mechanical modes of opto-mechanical system coupled to a three-level atom in cascade configuration, for any operator $\hat{O}$, the Heisenberg Equation of Motion is:

$$\frac{d\hat{O}_k}{dt} = \frac{i}{\hbar}[\hat{H}_{int}, \hat{O}_k] - \frac{\gamma_k}{2}\hat{O}_k \tag{5}$$

The Heisenberg Equation of three level atomic mode interaction with two mode cavity light is:

$$\frac{d\hat{a}_1}{dt} = -\frac{g}{\hbar}\sigma_{21} - \frac{\kappa}{2}\hat{a}_1, \quad \frac{d\hat{a}_2}{dt} = -\frac{g}{\hbar}\sigma_{32} - \frac{\kappa}{2}\hat{a}_2. \tag{6}$$

In the bad-cavity limit ($\kappa \gg g$), we can adiabatically eliminate the cavity modes, leading to the steady-state relationship between the field and atomic operators.

$$\begin{aligned}\hat{a}_1 = -\frac{2g}{\kappa}\hat{\sigma}_{21}, \quad \hat{a}_2 = -\frac{2g}{\kappa}\hat{\sigma}_{32}, \quad \hat{a}_1^\dagger\hat{a}_1 = \frac{4g^2}{\kappa^2}\hat{\sigma}_{11}\\ \hat{a}_1\hat{a}_1^\dagger = \frac{4g^2}{\kappa^2}\hat{\sigma}_{22}, \quad \hat{a}_2^\dagger\hat{a}_2 = \frac{4g^2}{\kappa^2}\hat{\sigma}_{22}, \quad \hat{a}_2\hat{a}_2^\dagger = \frac{4g^2}{\kappa^2}\hat{\sigma}_{33}. \end{aligned} \tag{7}$$

Rising, lowering and population of atomic operators determined from Eq. (7) and their complex conjugate as:

$$\begin{aligned}\hat{\sigma}_{21} = -\frac{\kappa}{2g}\hat{a}_1, \quad \hat{\sigma}_{32} = -\frac{\kappa}{2g}\hat{a}_2, \quad \hat{\sigma}_{11} = \frac{\kappa^2}{4g^2}\hat{a}_1^\dagger\hat{a}_1\\ \hat{\sigma}_{13} = \frac{\kappa^2}{4g^2}\hat{a}_1^\dagger\hat{a}_2^\dagger, \quad \hat{\sigma}_{33} = \frac{\kappa^2}{4g^2}\hat{a}_2\hat{a}_2^\dagger, \quad \hat{\sigma}_{22} = \frac{\kappa^2}{4g^2}\hat{a}_2^\dagger\hat{a}_2. \end{aligned} \tag{8}$$

The Heisenberg Equation for the two modes mechanical operator interaction with cavity mode is:

$$\frac{d\hat{b}_i}{dt} = ig_{0_i}\hat{a}_i^\dagger\hat{a}_i - \frac{\gamma_m}{2}\hat{b}_i, \tag{9}$$

where as the mechanical mode evolves under the radiation pressure force proportional to the cavity photon number, and decays at rate γ_m, the steady-state solution of the mechanical annihilation operator:

$$\hat{b}_j = \frac{2ig_{0_j}}{\gamma_m}\hat{a}_j^\dagger\hat{a}_j. \tag{10}$$

The above solution is an operator relation, not an observable thus mechanical annihilation operator $\hat{b}_j$ is fundamentally non-Hermitian.Then the phonon number of mechanical mode with aid of Eq. (10) given as:

$$\hat{b}_j^\dagger\hat{b}_j = \hat{b}_j\hat{b}_j^\dagger = \frac{4g_{0_j}^2}{\gamma_m^2}\left(\hat{a}_j^{\dagger 2}\hat{a}_j^2 + 2\hat{a}_j^\dagger\hat{a}_j\right). \tag{11}$$

For $X_i = g_{0i}(\hat{b}_i + \hat{b}_i^\dagger)$ but $\hat{b}_i = \frac{2ig_{0_i}}{\gamma_m}\hat{a}_i^\dagger\hat{a}_i = \frac{2ig_{0_i}}{\gamma_m}\hat{n}_i$ and $\hat{b}_i^\dagger = -\frac{2ig_{0_i}}{\gamma_m}(\hat{n}_i + 1)$ therefore:

$$X_i = -\frac{2ig_{0i}^2}{\gamma_m}. \tag{12}$$

The single-photon optomechanical cooperativity is defined as

$$C_{0_i} = \frac{4g_{0_i}^2}{\kappa\gamma_m}, \tag{13}$$

where g_{0_i} denotes the single-photon optomechanical coupling strength, κ is the cavity decay rate, and γ_m is the mechanical damping rate. This dimensionless parameter quantifies the competition between coherent optomechanical interaction and dissipative processes and determines access to the single-photon strong-coupling regime [27]. In most current cavity optomechanical experiments, however, the single-photon coupling remains weak $C_0 \ll 1$, and strong interaction effects are typically achieved via intracavity field enhancement in the linearized regime [27, 29, 30].
With the aid of Eq. (113), Eq. (12) re-written as:

$$X_i = -\frac{i\kappa}{2}C_{0_i}. \tag{14}$$

Master equation of the system given by Eq. (4) in the terms given as cavity mode using the Eq. (10), Eq. (11), Eq. (113), Eq. (14)

$$\begin{aligned}\frac{d\hat{\rho}}{dt} &= \frac{1}{2}\Big(\kappa(N+1)+\frac{\gamma\kappa}{2\gamma_c}\Big)\Big([\hat{a}_1,\rho\hat{a}_1^\dagger]+[\hat{a}_1\rho,\hat{a}_1^\dagger]\Big)+\frac{1}{2}\big(\kappa N+G\rho_{11}^{(0)}\big)\Big([\hat{a}_1^\dagger,\rho\hat{a}_1]+[\hat{a}_1^\dagger\rho,\hat{a}_1]\Big)\\
&+\frac{1}{2}\Big(\kappa(N+1)+\frac{\gamma\kappa}{2\gamma_c}+G\rho_{33}^{(0)}\Big)\Big([\hat{a}_2,\rho\hat{a}_2^\dagger]+[\hat{a}_2\rho,\hat{a}_2^\dagger]\Big)+\frac{\kappa N}{2}\Big([\hat{a}_2^\dagger,\rho\hat{a}_2]+[\hat{a}_2^\dagger\rho,\hat{a}_2]\Big)\\
&-\Big(\frac{G\rho_{13}^{(0)}}{2}+\kappa M_a\Big)\Big([\hat{a}_1^\dagger,\rho\hat{a}_2^\dagger]+[\hat{a}_1^\dagger\rho,\hat{a}_2^\dagger]\Big)-\Big(\frac{G\rho_{31}^{(0)}}{2}+\kappa M_a\Big)\Big([\hat{a}_2,\rho\hat{a}_1]+[\hat{a}_2\rho,\hat{a}_1]\Big)\\
&-\kappa M_a\Big([\hat{a}_2^\dagger,\rho\hat{a}_1^\dagger]+[\hat{a}_1,\rho\hat{a}_2]\Big)+iX_1[\hat{a}_1^\dagger\hat{a}_1,\ \hat{\rho}]+iX_2[\hat{a}_2^\dagger\hat{a}_2,\ \hat{\rho}]\\
&+C_{0_1}\kappa(n_{th,1}+1)\Big([\hat{a}_1^\dagger\hat{a}_1,\ \hat{\rho}\hat{a}_1\hat{a}_1^\dagger]+[\hat{a}_1^\dagger\hat{a}_1\hat{\rho},\ \hat{a}_1\hat{a}_1^\dagger]\Big)+C_{0_1}\kappa n_{th,1}\Big([\hat{a}_1\hat{a}_1^\dagger,\ \hat{\rho}\hat{a}_1^\dagger\hat{a}_1]+[\hat{a}_1\hat{a}_1^\dagger\hat{\rho},\ \hat{a}_1^\dagger\hat{a}_1]\Big)\\
&+C_{0_2}\kappa(n_{th,2}+1)\Big([\hat{a}_2^\dagger\hat{a}_2\hat{,}\ \rho\hat{a}_2\hat{a}_2^\dagger]+[\hat{a}_2^\dagger\hat{a}_2\hat{\rho},\ \hat{a}_2\hat{a}_2^\dagger]\Big)+C_{0_2}\kappa n_{th,2}\Big([\hat{a}_2\hat{a}_2^\dagger,\ \hat{\rho}\hat{a}_2^\dagger\hat{a}_2]+[\hat{a}_2\hat{a}_2^\dagger\hat{\rho},\ \hat{a}_2^\dagger\hat{a}_2]\Big).\end{aligned}\tag{15}$$

Let define terms as:

$$\begin{aligned}\mu_1=\tfrac{1}{2}\Big(\kappa(N+1)+\frac{\gamma\kappa}{2\gamma_c}\Big),\quad \mu_3=\tfrac{1}{2}\big(\kappa N+G\rho_{11}^{(0)}\big),\quad \mu_2=\tfrac{1}{2}\Big(\kappa(N+1)+\frac{\gamma\kappa}{2\gamma_c}+G\rho_{33}^{(0)}\Big),\quad \mu_4=\tfrac{\kappa N}{2}\\
\nu_1=\kappa M_a,\quad \nu_2=\frac{G\rho_{13}^{(0)}}{2}+\kappa M_a=\frac{G\rho_{13}^{(0)}}{2}+\nu_1,\quad \nu_3=\frac{G\rho_{31}^{(0)}}{2}+\kappa M_a=\frac{G\rho_{31}^{(0)}}{2}+\nu_1\\
N_1=\tfrac{C_{0_1}\kappa}{2}-\mu_1,\quad N_2=\tfrac{C_{0_1}\kappa}{2}+\mu_1,\quad \nu_4=\kappa C_{0_1},\quad \nu_5=\kappa C_{0_2}\\
T_1=C_{0_1}\kappa(n_{th,1}+1),\quad T_2=C_{0_1}\kappa n_{th,1},\quad T_3=C_{0_2}\kappa(n_{th,2}+1),\quad T_4=C_{0_2}\kappa n_{th,2}.\end{aligned}\tag{16}$$

Master equation of the system given by Eq (15) using the definition of Eq ():

$$\begin{aligned}\frac{d\hat{\rho}}{dt} &= \mu_1\Big([\hat{a}_1,\ \rho\hat{a}_1^\dagger]+[\hat{a}_1\rho,\ \hat{a}_1^\dagger]\Big)+\mu_3\Big([\hat{a}_1^\dagger,\ \rho\hat{a}_1]+[\hat{a}_1^\dagger\rho,\ \hat{a}_1]\Big)+\mu_2\Big([\hat{a}_2,\rho\hat{a}_2^\dagger]+[\hat{a}_2\rho,\ \hat{a}_2^\dagger]\Big)\\
&+\mu_4\Big([\hat{a}_2^\dagger,\ \rho\hat{a}_2]+[\hat{a}_2^\dagger\rho,\ \hat{a}_2]\Big)-\nu_2\Big([\hat{a}_1^\dagger,\ \rho\hat{a}_2^\dagger]+[\hat{a}_1^\dagger\rho,\ \hat{a}_2^\dagger]\Big)-\nu_3\Big([\hat{a}_2,\ \rho\hat{a}_1]+[\hat{a}_2\rho,\ \hat{a}_1]\Big)\\
&+T_1\big([\hat{a}_1^\dagger\hat{a}_1,\ \rho\hat{a}_1\hat{a}_1^\dagger]+[\hat{a}_1^\dagger\hat{a}_1\rho,\ \hat{a}_1\hat{a}_1^\dagger]\big)+T_2\Big([\hat{a}_1\hat{a}_1^\dagger,\ \rho\hat{a}_1^\dagger\hat{a}_1]+[\hat{a}_1\hat{a}_1^\dagger\rho,\ \hat{a}_1^\dagger\hat{a}_1]\Big)\\
&+T_3\Big([\hat{a}_2^\dagger\hat{a}_2,\ \rho\hat{a}_2\hat{a}_2^\dagger]+[\hat{a}_2^\dagger\hat{a}_2\rho,\ \hat{a}_2\hat{a}_2^\dagger]\Big)+T_4\Big([\hat{a}_2\hat{a}_2^\dagger,\ \rho\hat{a}_2^\dagger\hat{a}_2]+[\hat{a}_2\hat{a}_2^\dagger\rho,\ \hat{a}_2^\dagger\hat{a}_2]\Big)\\
&-\nu_1\big([\hat{a}_2^\dagger,\ \rho\hat{a}_1^\dagger]+[\hat{a}_1,\ \rho\hat{a}_2]\big)+\frac{\nu_4}{2}\big([\hat{a}_1^\dagger\hat{a}_1,\ \rho]\big)+\frac{\nu_5}{2}\big([\hat{a}_2^\dagger\hat{a}_2,\ \rho]\big)\end{aligned}\tag{17}$$

2.2. Expectation Values of Cavity Mode Variables

Applying the relation $\frac{d\langle\hat{A}\rangle}{dt}=Tr\Big(\frac{d\hat{\rho}}{dt}\hat{A}\Big)$ along with Eq. (17) and the cyclic property of the trace operation, we can write

$$\begin{aligned}\frac{d}{dt}\langle\hat{A}\rangle &= \mu_1\ \mathrm{Tr}\Big([\hat{a}_1,\ \rho\hat{a}_1^\dagger]\hat{A}+[\hat{a}_1\rho,\ \hat{a}_1^\dagger]\hat{A}\Big)+\mu_3\ \mathrm{Tr}\Big([\hat{a}_1^\dagger,\ \rho\hat{a}_1]\hat{A}+[\hat{a}_1^\dagger\rho,\ \hat{a}_1]\hat{A}\Big)\\
&+\mu_2\ \mathrm{Tr}\Big([\hat{a}_2,\rho\hat{a}_2^\dagger]\hat{A}+[\hat{a}_2\rho,\ \hat{a}_2^\dagger]\hat{A}\Big)+\mu_4\ \mathrm{Tr}\Big([\hat{a}_2^\dagger,\ \rho\hat{a}_2]\hat{A}+[\hat{a}_2^\dagger\rho,\ \hat{a}_2]\hat{A}\Big)\\
&-\nu_2\ \mathrm{Tr}\Big([\hat{a}_1^\dagger,\ \rho\hat{a}_2^\dagger]\hat{A}+[\hat{a}_1^\dagger\rho,\ \hat{a}_2^\dagger]\hat{A}\Big)-\nu_3\ \mathrm{Tr}\Big([\hat{a}_2,\ \rho\hat{a}_1]\hat{A}+[\hat{a}_2\rho,\ \hat{a}_1]\hat{A}\Big)\\
&-\nu_1\ \mathrm{Tr}\Big([\hat{a}_2^\dagger,\ \rho\hat{a}_1^\dagger]\hat{A}+[\hat{a}_1,\ \rho\hat{a}_2]\hat{A}\Big)+iX_1\ \mathrm{Tr}\big([\hat{a}_1^\dagger\hat{a}_1,\ \rho]\hat{A}\big)+iX_2\ \mathrm{Tr}\big([\hat{a}_2^\dagger\hat{a}_2,\ \rho]\hat{A}\big)\\
&+T_1\ \mathrm{Tr}\Big([\hat{a}_1^\dagger\hat{a}_1,\ \rho\hat{a}_1\hat{a}_1^\dagger]\hat{A}+[\hat{a}_1^\dagger\hat{a}_1\rho,\ \hat{a}_1\hat{a}_1^\dagger]\hat{A}\Big)+T_2\ \mathrm{Tr}\Big([\hat{a}_1\hat{a}_1^\dagger,\ \rho\hat{a}_1^\dagger\hat{a}_1]\hat{A}+[\hat{a}_1\hat{a}_1^\dagger\rho,\ \hat{a}_1^\dagger\hat{a}_1]\hat{A}\Big)\\
&+T_3\ \mathrm{Tr}\Big([\hat{a}_2^\dagger\hat{a}_2,\ \rho\hat{a}_2\hat{a}_2^\dagger]\hat{A}+[\hat{a}_2^\dagger\hat{a}_2\rho,\ \hat{a}_2\hat{a}_2^\dagger]\hat{A}\Big)+T_4\ \mathrm{Tr}\Big([\hat{a}_2\hat{a}_2^\dagger,\ \rho\hat{a}_2^\dagger\hat{a}_2]\hat{A}+[\hat{a}_2\hat{a}_2^\dagger\rho,\ \hat{a}_2^\dagger\hat{a}_2]\hat{A}\Big)\end{aligned}\tag{18}$$

With aid of Eq. (18), second moments of bosonic field operators, let find equations of motion at steady state, all time derivatives vanish:

$$\begin{aligned} 0 &= (\mu_a + iX_1 - \nu_a)\langle \hat{a}_1 \rangle - \nu_2 \langle \hat{a}_2^\dagger \rangle \\ 0 &= (\mu_b + iX_2 - \nu_b)\langle \hat{a}_2 \rangle + (\nu_2 - \nu_1)\langle \hat{a}_1^\dagger \rangle \end{aligned} \tag{19}$$

Eq. (19) shows that:

$$\langle \hat{a}_1 \rangle = \hat{a}_2^\dagger \rangle = \langle \hat{a}_2 \rangle = \langle \hat{a}_1^\dagger \rangle = 0 \tag{20}$$

$$\begin{aligned} \langle \hat{a}_1^2 \rangle &= \frac{\nu_2}{D_1} \langle a_2^\dagger a_1 \rangle \\ \langle \hat{a}_2^{\dagger 2} \rangle &= -\frac{\nu_3}{D_2^*} \langle \hat{a}_2^\dagger \hat{a}_1 \rangle \end{aligned} \tag{21}$$

$$\begin{aligned} \langle \hat{a}_2^2 \rangle &= \frac{-\nu_2 \langle a_2 a_1^\dagger \rangle + \nu_1 \langle a_1^\dagger a_2 \rangle}{D_2} \\ \langle \hat{a}_1^{\dagger 2} \rangle &= \frac{\nu_3 \langle \hat{a}_1^\dagger \hat{a}_2 \rangle - \nu_1 \langle \hat{a}_2 \hat{a}_1^\dagger \rangle}{D_1^*} \end{aligned} \tag{22}$$

Eq. (21), Eq. (22) shows that:

$$\langle \hat{a}_1^{\dagger 2} \rangle = \langle \hat{a}_2^2 \rangle = \langle \hat{a}_2^{\dagger 2} \rangle = \langle \hat{a}_1^2 \rangle = 0 \tag{23}$$

With possible substitution Eq. (21), Eq. (22)becomes

$$\begin{aligned} \langle \hat{a}_2^\dagger \hat{a}_1 \rangle &= \frac{\mu_{34} D_1 D_2^*}{D_3^* D_1 D_2^* - \nu_2 \nu_3 (D_1 - D_2^*)} \langle \hat{a}_1 \hat{a}_2^\dagger \rangle \\ \langle \hat{a}_2 \hat{a}_1^\dagger \rangle &= \frac{D_1^* D_2 D_3 + \nu_{12_-} \nu_3 D_2 - \nu_{13_-} \nu_1 D_1^*}{\mu_{34} D_1^* D_2 + \nu_{12_-} \nu_1 D_2 - \nu_{13_-} \nu_2 D_1^*} \langle \hat{a}_1^\dagger \hat{a}_2 \rangle \end{aligned} \tag{24}$$

$$\langle \hat{a}_1^\dagger \hat{a}_1 \rangle = \frac{-2\mu_3 + \nu_2 \langle \hat{a}_2^\dagger \hat{a}_1^\dagger \rangle - \nu_{13_-} \langle \hat{a}_1 \hat{a}_2 \rangle}{2\mu_a} \tag{25}$$

$$\langle \hat{a}_2^\dagger \hat{a}_2 \rangle = \frac{-2\mu_4 + \nu_{12_-} \langle \hat{a}_2^\dagger \hat{a}_1^\dagger \rangle - \nu_3 \langle \hat{a}_1 \hat{a}_2 \rangle}{2\mu_b} \tag{26}$$

$$\langle \hat{a}_1^\dagger \hat{a}_2^\dagger \rangle = \langle \hat{a}_2^\dagger \hat{a}_1^\dagger \rangle = -\frac{\nu_3 \langle \hat{a}_1^\dagger \hat{a}_1 \rangle + \nu_{13_-} \langle \hat{a}_2^\dagger \hat{a}_2 \rangle + \nu_{13_+}}{D_+^*} \tag{27}$$

$$\langle a_1 a_2 \rangle = \langle a_2 a_1 \rangle = \frac{\nu_{12_-} \langle a_1^\dagger a_1 \rangle + \nu_2 (\langle a_2^\dagger a_2 \rangle - 1)}{D_+}. \tag{28}$$

Substituting Eq. (25), in to Eq. (27) and Eq. (26), in to Eq. (28)

$$\langle \hat{a}_1^\dagger \hat{a}_1 \rangle = \frac{-\nu_2 \nu_{13_-} (D_+ + D_+^*) \langle \hat{a}_2^\dagger \hat{a}_2 \rangle - \nu_2 \nu_{13_+} D_+ + \nu_2 \nu_{13_-} D_+^* - 2\mu_3 D_+ D_+^*}{2\mu_a D_+ D_+^* + \nu_2 \nu_3 D_+ + \nu_{13_-} \nu_{12_-} D_+^*} \tag{29}$$

$$\langle \hat{a}_2^\dagger \hat{a}_2 \rangle = \frac{-2\mu_4 D_+^* D_+ - \nu_{12_-} \nu_{13_+} D_+ - \nu_3 \nu_2 D_+^* - (\nu_{12_-} \nu_3 D_+ + \nu_3 \nu_{12_-} D_+^*) \langle \hat{a}_1^\dagger \hat{a}_1 \rangle}{2\mu_b D_+^* D_+ + \nu_{12_-} \nu_{13_-} D_+ + \nu_3 \nu_2 D_+^*}. \tag{30}$$

Substituting Eq. (29), in to Eq. (30)

$$\langle \hat{a}_2^\dagger \hat{a}_2 \rangle = \frac{-4\mu_4 \mu_a |D_+|^4 + \Big(2\mu_a A_3 - 2\mu_4 A_1\Big)|D_+|^2 + 4\nu_3 \nu_{13_-} \mu_3 |D_+|^2 \,\mathrm{Re} D_+ + A_3 A_1 - 2\nu_3 \nu_{13_-} A_2 \,\mathrm{Re} D_+}{4\mu_a \mu_b |D_+|^4 + 2\big(\mu_b A_1 + \mu_a A_1^*\big)|D_+|^2 + A_1^* A_1 - 4\nu_3^2 \nu_{13_-}^2 (\mathrm{Re} D_+)^2}. \tag{31}$$

Substituting Eq. (30), in to Eq. (29)

$$\langle \hat{a}_1^\dagger \hat{a}_1 \rangle = \frac{-4\mu_3 \mu_b |D_+|^4 + \Big(2\mu_b A_2 - 2\mu_3 A_1^*\Big)|D_+|^2 + 4\nu_3 \nu_{13_-} \mu_4 |D_+|^2 \,\mathrm{Re} D_+ + A_2 A_1^* - 2\nu_3 \nu_{13_-} A_4 \,\mathrm{Re} D_+}{4\mu_a \mu_b |D_+|^4 + 2\big(\mu_a A_1^* + \mu_b A_1\big)|D_+|^2 + A_1 A_1^* - 4\nu_3^2 \nu_{13_-}^2 (\mathrm{Re} D_+)^2}. \tag{32}$$

Substituting Eq. (31) and Eq. (32) in to Eq. (28)

$$\begin{aligned} \langle a_1 a_2 \rangle = {} & \frac{-4(\nu_{13_-} \mu_3 \mu_b + \nu_3 \mu_4 \mu_a + \nu_3 \mu_a \mu_b)|D_+|^4 + \nu_{13_-} A_2 A_1^* + \nu_3 A_3 A_1 - \nu_3 |A_1|^2}{D_+ \Big(4\mu_a \mu_b |D_+|^4 + (2\mu_a A_1^* + 2\mu_b A_1)|D_+|^2 + |A_1|^2 - 4\nu_3^2 \nu_{13_-}^2 (\mathrm{Re} D_+)^2\Big)} \\ & + \frac{|D_+|^2 \Big[2\nu_{13_-} \mu_b A_2 - 2\nu_{13_-} \mu_3 A_1^* + 2\nu_3 \mu_a A_3 - 2\nu_3 \mu_4 A_1 - 2\nu_3 \mu_a A_1^* - 2\nu_3 \mu_b A_1\Big]}{D_+ \Big(4\mu_a \mu_b |D_+|^4 + (2\mu_a A_1^* + 2\mu_b A_1)|D_+|^2 + |A_1|^2 - 4\nu_3^2 \nu_{13_-}^2 (\mathrm{Re} D_+)^2\Big)} \\ & + \frac{4\nu_{13_-} \nu_3 (\nu_{13_-} \mu_4 + \nu_3 \mu_3)|D_+|^2 \,\mathrm{Re} D_+ - 2\nu_{13_-} \nu_3 (\nu_{13_-} A_4 + \nu_3 A_2) \,\mathrm{Re} D_+ + 4\nu_3^3 \nu_{13_-}^2 (\mathrm{Re} D_+)^2}{D_+ \Big(4\mu_a \mu_b |D_+|^4 + (2\mu_a A_1^* + 2\mu_b A_1)|D_+|^2 + |A_1|^2 - 4\nu_3^2 \nu_{13_-}^2 (\mathrm{Re} D_+)^2\Big)}. \end{aligned} \tag{33}$$

Substituting Eq. (31) and Eq. (32) in to Eq. (27)

$$\begin{aligned}\langle \hat{a}_1^\dagger \hat{a}_2^\dagger \rangle = & \frac{4|D_+|^4\left(\nu_3\mu_3\mu_b + \nu_{13_-}\mu_a\mu_4 - \nu_{13_+}\mu_a\mu_b\right) + 4\nu_3^2\nu_{13_-}^2\nu_{13_+}(\mathrm{Re}D_+)^2}{D_+^*\left(4\mu_a\mu_b|D_+|^4 + 2|D_+|^2(\mu_a A_1^* + \mu_b A_1) + |A_1|^2 - 4\nu_3^2\nu_{13_-}^2(\mathrm{Re}D_+)^2\right)} \\ & - \frac{2|D_+|^2\left(\nu_3\mu_b A_2 - \nu_3\mu_3 A_1^* + \nu_{13_-}\mu_a A_3 - \nu_{13_-}\mu_4 A_1 + \nu_{13_+}\mu_a A_1^* + \nu_{13_+}\mu_b A_1\right)}{D_+^*\left(4\mu_a\mu_b|D_+|^4 + 2|D_+|^2(\mu_a A_1^* + \mu_b A_1) + |A_1|^2 - 4\nu_3^2\nu_{13_-}^2(\mathrm{Re}D_+)^2\right)} \\ & - \frac{\nu_3 A_2 A_1^* + \nu_{13_-}A_3 A_1 + \nu_{13_+}|A_1|^2 + 2\nu_3^2\nu_{13_-}(A_4 + A_2)\mathrm{Re}D_+}{D_+^*\left(4\mu_a\mu_b|D_+|^4 + 2|D_+|^2(\mu_a A_1^* + \mu_b A_1) + |A_1|^2 - 4\nu_3^2\nu_{13_-}^2(\mathrm{Re}D_+)^2\right)} \\ & - \frac{4|D_+|^2\nu_3\nu_{13_-}(\mu_4 + \mu_3)\mathrm{Re}D_+}{D_+^*\left(4\mu_a\mu_b|D_+|^4 + 2|D_+|^2(\mu_a A_1^* + \mu_b A_1) + |A_1|^2 - 4\nu_3^2\nu_{13_-}^2(\mathrm{Re}D_+)^2\right)}\end{aligned} \tag{34}$$

The anomalous correlations $\langle \hat{a}_i \hat{a}_j \rangle$ and $\langle \hat{a}_i^\dagger \hat{a}_j^\dagger \rangle$ are nonclassical, as they do not occur in classical light fields, coherent states, or thermal states. In this system, they arise from a nondegenerate three-level cascade laser, where an atom prepared in a coherent superposition $C_1|1\rangle + C_3|3\rangle$ undergoes cascade transitions $|1\rangle \rightarrow |2\rangle \rightarrow |3\rangle$, emitting correlated photons into two distinct modes and generating atomic coherence $\rho_{13}^{(0)}$, which imprints two-photon coherence onto the field, yielding nonzero $\langle \hat{a}_1 \hat{a}_2 \rangle$. From Eq. (24) although the corresponding coefficients are nonzero, the normal correlations vanish, such that

$$\langle \hat{a}_i^\dagger \hat{a}_j \rangle = \langle \hat{a}_j \hat{a}_i^\dagger \rangle = 0. \tag{35}$$

Where the vanishing of all $\langle \hat{a}_i^\dagger \hat{a}_j \rangle$, $i \neq j$ indicates zero first-order coherence between modes, caused by either lack of direct coupling, independent reservoirs, or system symmetry. Practically, this allows independent operation of cavity modes, which is useful in multi-channel quantum information processing, parallel quantum communication, and noise-resilient optomechanical setups [27, 28, 32, 33].
Each individual mode has no intrinsic single-mode squeezing or phase-sensitive coherence, there is no hidden squeezing noise.

But there is still:

$$\langle \hat{a}_i \hat{a}_j \rangle \neq 0 \tag{36}$$

Thus there is two-mode squeezing or entanglement which is crucial in optomechanics.

3. Quantum Fluctuation Analysis

Quadrature fluctuations of single-mode light refer to the quantum uncertainties in the quadrature operators of a single mode of the electromagnetic field,and they are also critical in multi-mode systems for entanglement studies. For single-mode light, understanding fluctuations sets the stage for analyzing correlations in multi-mode systems, since it provide the baseline against which multi-mode correlations are compared to detect entanglement. Let define the operators as:

$$\hat{a}_{j\pm} = \sqrt{\pm 1}(\hat{a}_j^\dagger \pm \hat{a}_j) \tag{37}$$

For the $+$ case $\sqrt{+1} = 1$ and $-$ case $\sqrt{-1} = i$ then:

$$\hat{a}_{j+} = \hat{a}_j^\dagger + \hat{a}_j, \quad \hat{a}_{j-} = i(\hat{a}_j^\dagger - \hat{a}_j) \tag{38}$$

Compute $\langle \hat{a}_{j\pm}\hat{a}_{j\pm} \rangle$ to determine quadrature variance:

$$\Delta a_{j\pm}^2 = \langle \hat{a}_{j\pm}\hat{a}_{j\pm} \rangle = \langle \hat{a}_{j\pm}^2 \rangle \tag{39}$$

which requires the expectation value of the squared operators.

$$\hat{a}_{j+}^2 = (\hat{a}_j^\dagger + \hat{a}_j)(\hat{a}_j^\dagger + \hat{a}_j) = \hat{a}_j^\dagger\hat{a}_j^\dagger + \hat{a}_j^\dagger\hat{a}_j + \hat{a}_j\hat{a}_j^\dagger + \hat{a}_j\hat{a}_j \tag{40}$$

Use the commutation relation $\hat{a}_j\hat{a}_j^\dagger = \hat{a}_j^\dagger\hat{a}_j + 1$:

$$\hat{a}_{j+}^2 = \hat{a}_j^\dagger\hat{a}_j^\dagger + 2\hat{a}_j^\dagger\hat{a}_j + \hat{a}_j\hat{a}_j + 1 \tag{41}$$

The expectation value is:

$$\langle \hat{a}_{j+}^2 \rangle = \langle \hat{a}_j^\dagger\hat{a}_j^\dagger \rangle + 2\langle \hat{a}_j^\dagger\hat{a}_j \rangle + \langle \hat{a}_j\hat{a}_j \rangle + 1 \tag{42}$$

Similarly the expectation value $\hat{a}_{j-}^2$ in normal order is:

$$\langle \hat{a}_{j-}^2 \rangle = -\langle \hat{a}_j^\dagger\hat{a}_j^\dagger \rangle + 2\langle \hat{a}_j^\dagger\hat{a}_j \rangle - \langle \hat{a}_j\hat{a}_j \rangle + 1 \tag{43}$$

Therefore the quadrature variance of Eq. (39) becomes:

$$\Delta a_{j\pm}^2 = \langle a_{j\pm}^2 \rangle = 1 \pm \langle \hat{a}_j^\dagger\hat{a}_j^\dagger \rangle + 2\langle \hat{a}_j^\dagger\hat{a}_j \rangle \pm \langle \hat{a}_j\hat{a}_j \rangle \tag{44}$$

$$\Delta a_{j_\pm}^2 = 1 + 2\langle \hat{a}_j^\dagger\hat{a}_j \rangle \tag{45}$$

Since $\langle \hat{a}_j^\dagger\hat{a}_j^\dagger \rangle = \langle \hat{a}_j\hat{a}_j \rangle = 0$, then for $j = 1, 2$

$$\begin{aligned}\Delta a_{1_\pm}^2 &= 1 + 2\langle \hat{a}_1^\dagger\hat{a}_1 \rangle \\ \Delta a_{2_\pm}^2 &= 1 + 2\langle \hat{a}_2^\dagger\hat{a}_2 \rangle\end{aligned} \tag{46}$$

Single-mode correlations vanish:

$$\langle \hat{a}_j \hat{a}_j \rangle = 0 \tag{47}$$

Cross-mode correlations survive:

$$\langle \hat{a}_1 \hat{a}_2 \rangle \neq 0 \tag{48}$$

Hence, no single-mode squeezing, but two-mode squeezing can exist.

3.1. Quantum Squeezing of Two-Mode Light

Quadrature squeezing constitutes a distinctly quantum optical phenomenon in which the uncertainty of one Hermitian field quadrature constructed from the photon annihilation and creation operators is reduced below the standard quantum limit at the expense of enhanced fluctuations in its conjugate variable, consistent with the Heisenberg uncertainty principle and unattainable within classical electromagnetism. This nonclassical redistribution of noise, fundamental to precision enhanced quantum metrology and emerging photonic technologies, is characterized in a two-mode field through the quadrature operators defined as

$$\hat{c}_{\pm} = \sqrt{\pm 1}(\hat{c}^{\dagger} \pm \hat{c}) \tag{49}$$

where

$$\hat{c} = \hat{a}_1 + \hat{a}_2 \tag{50}$$

with $\hat{a}_1$ and $\hat{a}_2$ as annihilation operators for the two modes, are characterized by the variances of two Hermitian quadrature operators.

$$\hat{c}_+ = \hat{a}_1 + \hat{a}_1^{\dagger} + \hat{a}_2 + \hat{a}_2^{\dagger}, \quad \hat{c}_- = i(\hat{a}_1^{\dagger} - \hat{a}_1 + \hat{a}_2^{\dagger} - \hat{a}_2) \tag{51}$$

Then compute $\hat{c}_+^2$ by expanding the square:

$$\hat{c}_+^2 = \sum_{i=1}^{2}\sum_{j=1}^{2}\left(\hat{a}_i\hat{a}_j + \hat{a}_i^{\dagger}\hat{a}_j^{\dagger}\right) + \sum_{i\neq j}\left(\hat{a}_i\hat{a}_j^{\dagger} + \hat{a}_i^{\dagger}\hat{a}_j\right) + 2\sum_{i=1}^{2}\hat{a}_i^{\dagger}\hat{a}_i + 2 \tag{52}$$

Use the commutators only where necessary:

$$\hat{a}_i\hat{a}_i^{\dagger} = \hat{a}_i^{\dagger}\hat{a}_i + [\hat{a}_i, \hat{a}_i^{\dagger}] = \hat{a}_i^{\dagger}\hat{a}_i + 1 \quad (i = 1, 2), \tag{53}$$

Let take expectation values in the normal-ordered form becomes:

$$\langle \hat{c}_+^2 \rangle = \sum_{i=1}^{2}\sum_{j=1}^{2}\left(\langle \hat{a}_i\hat{a}_j \rangle + \langle \hat{a}_i^{\dagger}\hat{a}_j^{\dagger} \rangle\right) + \sum_{i\neq j}\left(\langle \hat{a}_i\hat{a}_j^{\dagger} \rangle + \langle \hat{a}_i^{\dagger}\hat{a}_j \rangle\right) + 2\sum_{i=1}^{2}\langle \hat{a}_i^{\dagger}\hat{a}_i \rangle + 2 \tag{54}$$

Compute the variance

$$\Delta c_+^2 = \langle \hat{c}_+^2 \rangle - \langle \hat{c}_+ \rangle^2 \tag{55}$$

where $\langle \hat{c}_+ \rangle^2 = 0$, and with the aid of Eq. (54) variance of plus quadrature becomes:

$$\Delta c_+^2 = 2\sum_{i=1}^{2}\sum_{j=1}^{2}\langle \hat{a}_i\hat{a}_j \rangle + 2\sum_{i=1}^{2}\sum_{j=1}^{2}\langle \hat{a}_i^{\dagger}\hat{a}_j^{\dagger} \rangle + 2\sum_{i\neq j}\left(\langle \hat{a}_i\hat{a}_j^{\dagger} \rangle + \langle \hat{a}_i^{\dagger}\hat{a}_j \rangle\right) + 2\sum_{i=1}^{2}\langle \hat{a}_i^{\dagger}\hat{a}_i \rangle + 2 \tag{56}$$

That of minus quadrature expressed as

$$\hat{c}_- = i\big(\hat{a}_1^{\dagger} - \hat{a}_1 + \hat{a}_2^{\dagger} - \hat{a}_2\big) \tag{57}$$

$$\hat{c}_-^2 = -\sum_{i=1}^{2}\sum_{j=1}^{2}\left(\hat{a}_i\hat{a}_j + \hat{a}_i^{\dagger}\hat{a}_j^{\dagger}\right) + \sum_{i=1}^{2}\left(\hat{a}_i^{\dagger}\hat{a}_i + \hat{a}_i\hat{a}_i^{\dagger}\right) - 2\sum_{i\neq j}\left(\hat{a}_i^{\dagger}\hat{a}_j + \hat{a}_i\hat{a}_j^{\dagger}\right) \tag{58}$$

Taking the expectation value we have:

$$\langle \hat{c}_-^2 \rangle = -2\sum_{i=1}^{2}\sum_{j=1}^{2}\langle \hat{a}_i\hat{a}_j \rangle - 2\sum_{i=1}^{2}\sum_{j=1}^{2}\langle \hat{a}_i^{\dagger}\hat{a}_j^{\dagger} \rangle + 2\sum_{i\neq j}\left(\langle \hat{a}_i^{\dagger}\hat{a}_j \rangle + \langle \hat{a}_i\hat{a}_j^{\dagger} \rangle\right) + 2\sum_{i=1}^{2}\langle \hat{a}_i^{\dagger}\hat{a}_i \rangle + 2 \tag{59}$$

Compute the variance of minus quadrature

$$\Delta c_-^2 = \langle \hat{c}_-^2 \rangle - \langle \hat{c}_- \rangle^2 \tag{60}$$

Mean of $\hat{c}_- = 0$ and substituting Eq. (59) in to Eq. (60) variance takes the form of:

$$\Delta c_-^2 = 2 + 2\left[\langle \hat{a}_1^{\dagger}\hat{a}_1 \rangle + \langle \hat{a}_2^{\dagger}\hat{a}_2 \rangle + \langle \hat{a}_1^{\dagger}\hat{a}_2 \rangle + \langle \hat{a}_1\hat{a}_2^{\dagger} \rangle\right] - 2\left[\left(\langle \hat{a}_1^2 \rangle + \langle \hat{a}_2^2 \rangle + \langle \hat{a}_1^{\dagger}\hat{a}_2^{\dagger} \rangle + \langle \hat{a}_1\hat{a}_2 \rangle\right)\right] \tag{61}$$

There fore using Eq. (56)and Eq. (61) we have:

$$\Delta c_{\pm}^2 = 2 \pm 2\langle \hat{a}_1^2 \rangle \pm 2\langle \hat{a}_2^2 \rangle + 2\langle \hat{a}_1^{\dagger}\hat{a}_1 \rangle + 2\langle \hat{a}_2^{\dagger}\hat{a}_2 \rangle \pm 2\langle \hat{a}_1^{\dagger}\hat{a}_2^{\dagger} \rangle + 2\langle \hat{a}_1^{\dagger}\hat{a}_2 \rangle + 2\langle \hat{a}_1\hat{a}_2^{\dagger} \rangle \pm 2\langle \hat{a}_1\hat{a}_2 \rangle \tag{62}$$

From Eq. (23) and Eq. (35), Eq. (3.1), reduced to:

$$\Delta c_{\pm}^2 = 2 + 2\left(\left[\langle \hat{a}_1^{\dagger}\hat{a}_1 \rangle + \langle \hat{a}_2^{\dagger}\hat{a}_2 \rangle\right] \pm \left[\langle \hat{a}_1^{\dagger}\hat{a}_2^{\dagger} \rangle + \langle \hat{a}_1\hat{a}_2 \rangle\right]\right) \tag{63}$$

$$
\begin{aligned}
\Delta c_{\pm}^{2} &= 2-\frac{8(\mu_4\mu_a+\mu_3\mu_b)|D_+|^4}{4\mu_a\mu_b|D_+|^4+2(\mu_aA_1^*+\mu_bA_1)|D_+|^2+|A_1|^2-4\nu_3^2\nu_{13_-}^2(\mathrm{Re}D_+)^2}\\
&+\frac{2\left(2(\mu_aA_3+\mu_bA_2)-2(\mu_4A_1+\mu_3A_1^*)+4\nu_3\nu_{13_-}(\mu_3+\mu_4)\mathrm{Re}D_+\right)|D_+|^2}{4\mu_a\mu_b|D_+|^4+2(\mu_aA_1^*+\mu_bA_1)|D_+|^2+|A_1|^2-4\nu_3^2\nu_{13_-}^2(\mathrm{Re}D_+)^2}\\
&\pm\frac{8\Big[D_+\big(\nu_3\mu_3\mu_b+\nu_{13_-}\mu_a\mu_4-\nu_{13_+}\mu_a\mu_b\big)-D_+^*\big(\nu_{13_-}\mu_3\mu_b+\nu_3\mu_4\mu_a+\nu_3\mu_a\mu_b\big)\Big]|D_+|^2}{4\mu_a\mu_b|D_+|^4+2(\mu_aA_1^*+\mu_bA_1)|D_+|^2+|A_1|^2-4\nu_3^2\nu_{13_-}^2(\mathrm{Re}D_+)^2}\\
&+\frac{2(A_3A_1+A_2A_1^*)-4\nu_3\nu_{13_-}(A_2+A_4)\mathrm{Re}D_+}{4\mu_a\mu_b|D_+|^4+2(\mu_aA_1^*+\mu_bA_1)|D_+|^2+|A_1|^2-4\nu_3^2\nu_{13_-}^2(\mathrm{Re}D_+)^2}\\
&\mp\frac{4D_+^*\Big[\nu_{13_-}\mu_3A_1^*+\nu_3\mu_4A_1+\nu_3\mu_aA_1^*+\nu_3\mu_bA_1\Big]}{4\mu_a\mu_b|D_+|^4+2(\mu_aA_1^*+\mu_bA_1)|D_+|^2+|A_1|^2-4\nu_3^2\nu_{13_-}^2(\mathrm{Re}D_+)^2}\\
&\pm\frac{4D_+^*\Big[\nu_{13_-}\mu_bA_2+\nu_3\mu_aA_3+2\nu_{13_-}\nu_3(\nu_{13_-}\mu_4+\nu_3\mu_3)\mathrm{Re}D_+\Big]}{4\mu_a\mu_b|D_+|^4+2(\mu_aA_1^*+\mu_bA_1)|D_+|^2+|A_1|^2-4\nu_3^2\nu_{13_-}^2(\mathrm{Re}D_+)^2}\\
&\mp\frac{4D_+\Big[\nu_3\mu_bA_2+\nu_{13_-}\mu_aA_3+2\nu_3\nu_{13_-}(\mu_4+\mu_3)\mathrm{Re}D_+\Big]}{4\mu_a\mu_b|D_+|^4+2(\mu_aA_1^*+\mu_bA_1)|D_+|^2+|A_1|^2-4\nu_3^2\nu_{13_-}^2(\mathrm{Re}D_+)^2}\\
&\pm\frac{4D_+\Big[\nu_3\mu_3A_1^*+\nu_{13_-}\mu_4A_1-\nu_{13_+}\mu_aA_1^*-\nu_{13_+}\mu_bA_1\Big]}{4\mu_a\mu_b|D_+|^4+2(\mu_aA_1^*+\mu_bA_1)|D_+|^2+|A_1|^2-4\nu_3^2\nu_{13_-}^2(\mathrm{Re}D_+)^2}\\
&\pm\frac{2\left(\nu_{13_-}A_2A_1^*+\nu_3A_3A_1-\nu_3|A_1|^2-2\nu_{13_-}\nu_3(\nu_{13_-}A_4+\nu_3A_2)\mathrm{Re}D_++4\nu_3^3\nu_{13_-}^2(\mathrm{Re}D_+)^2\right)}{D_+\left(4\mu_a\mu_b|D_+|^4+2(\mu_aA_1^*+\mu_bA_1)|D_+|^2+|A_1|^2-4\nu_3^2\nu_{13_-}^2(\mathrm{Re}D_+)^2\right)}\\
&\mp\frac{2\left(\nu_3A_2A_1^*+\nu_{13_-}A_3A_1+\nu_{13_+}|A_1|^2+2\nu_3^2\nu_{13_-}(A_4+A_2)\mathrm{Re}D_+-4\nu_3^2\nu_{13_-}^2\nu_{13_+}(\mathrm{Re}D_+)^2\right)}{D_+^*\left(4\mu_a\mu_b|D_+|^4+2(\mu_aA_1^*+\mu_bA_1)|D_+|^2+|A_1|^2-4\nu_3^2\nu_{13_-}^2(\mathrm{Re}D_+)^2\right)}
\end{aligned}
\tag{64}
$$

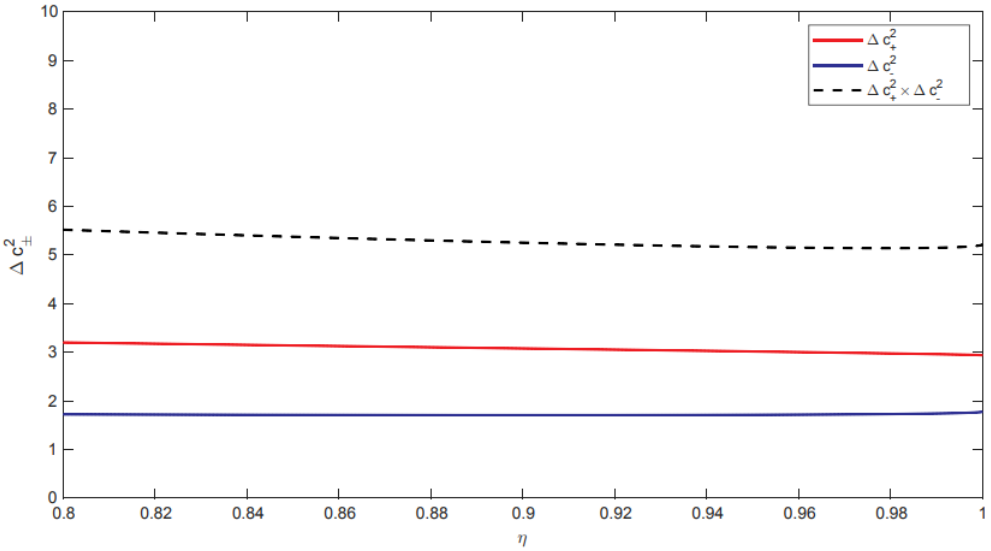

Figure 2. *Plots of* $\Delta c_{\pm}$ *[Eq (64)] versus* η *for* $\kappa = 0.8\, r = 0.5$, $\gamma_c = 0.01, C_{0_1} = C_{0_3} = 10^{-3}$, $n_{th_1} = n_{th_2} = 10^3$, $\gamma = 0.1$; *and* $G = 1$.

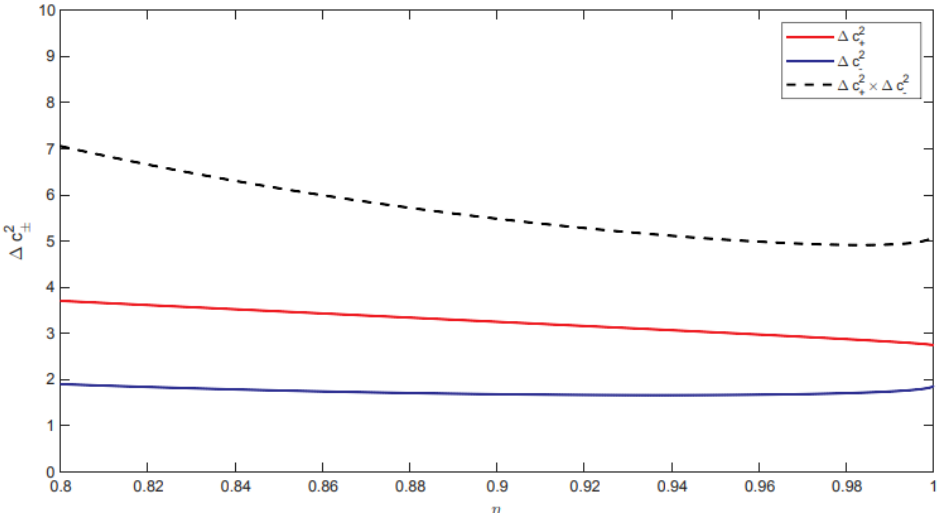

Figure 3. *Plots of* $\Delta c_\pm$ *[Eq* (64)*] versus* η *for* $\kappa = 0.8$ $r = 0.5$, $\gamma_c = 0.01$,$C_{0_1} = C_{0_3} = 10^{-3}$, $n_{th_1} = n_{th_2} = 10^3$, $\gamma = 0.1$*; and* $G = 4.5$.

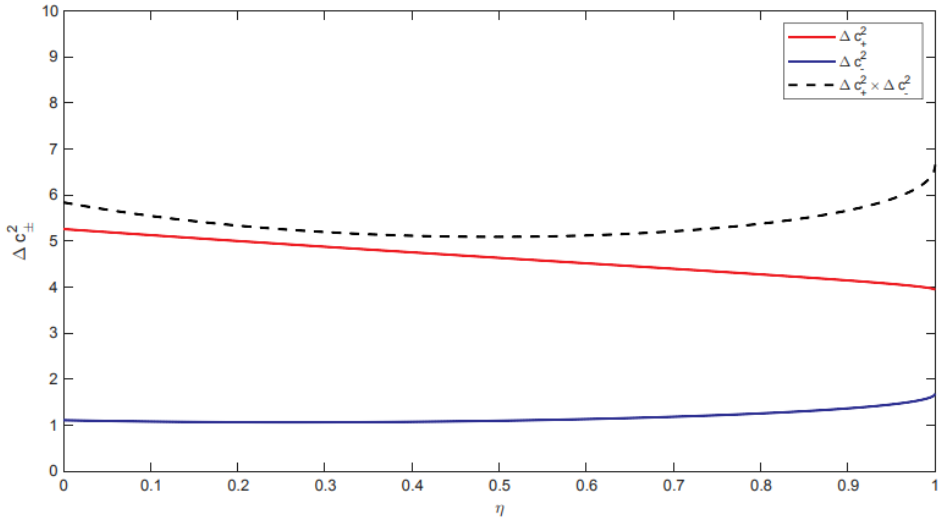

Figure 4. *Plots of* $\Delta c_\pm$ *[Eq* (64)*] versus* η *for* $\kappa = 0.8$ $r = 1.0$, $\gamma_c = 0.01$,$C_{0_1} = C_{0_3} = 10^{-3}$, $n_{th_1} = n_{th_2} = 10^3$, $\gamma = 0.1$*; and* $G = 1$.

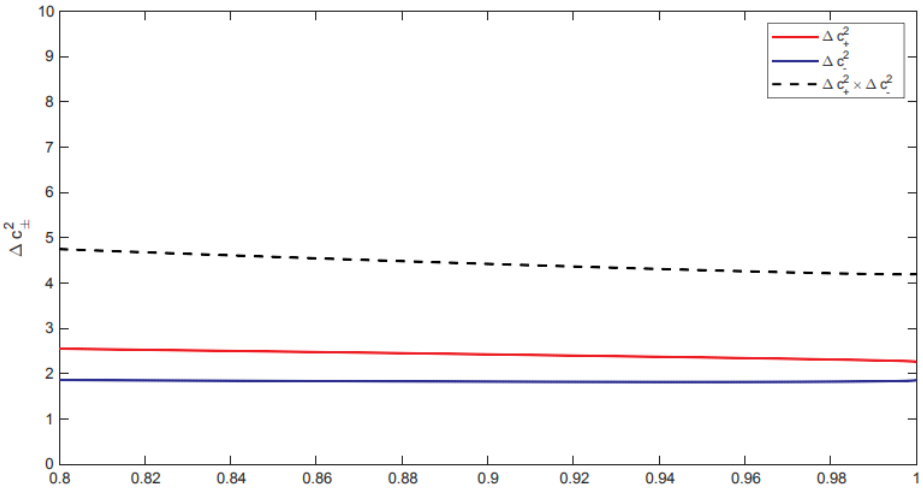

Figure 5. *Plots of* $\Delta c_\pm$ *[Eq.* (64)*] versus* η *for* $\kappa = 0.8$, $r = 0.25$, $\gamma_c = 0.01$, $C_{0_1} = C_{0_3} = 10^{-3}$, $n_{th_1} = n_{th_2} = 10^3$, $\gamma = 0.1$, *and* $G = 1$.

From the Figs. 2–5, the minus quadrature Δc_-^2 (blue solid line) represents the squeezed component in all plots and remains near or below the vacuum threshold of 2, indicating suppression of quantum noise. The plus quadrature Δc_+^2 (red solid line) represents the anti-squeezed component and remains above 2, absorbing the noise transferred from the minus quadrature to satisfy quantum mechanical constraints. The variance product (black dashed line) corresponds to the uncertainty product $\Delta c_+^2 \times \Delta c_-^2$ and remains at or above the vacuum limit (typically 4 in this scaling), confirming compliance with the Heisenberg Uncertainty Principle while redistributing noise.

A comparison of Figure 4($r = 1.0$) and Figure 5 ($r = 0.25$) shows that higher r significantly enhances squeezing and that the system maintains squeezing even at $n_{\text{th}} = 10^3$, which typically destroys quantum effects in other systems. Unlike traditional models, squeezing is achieved at low gain ($G = 1$), and although increasing the gain to $G = 4.5$ enhances anti-squeezing, it does not eliminate squeezing, which persists even at very weak coupling ($C_0 = 10^{-3}$), thereby facilitating experimental realization. According to [31], squeezing is fragile and strongly dependent on population inversion (η), whereas the present system exhibits only weak dependence on η, relies on reservoir-induced correlations rather than heat-sensitive atomic coherence, and does not require large atomic gain or high power to overcome thermal noise, thereby enhancing its practical robustness.

The pump-free operation arises because the squeezed vacuum reservoir functions as a pre-correlated environment, enabling the atoms and mechanical resonator to inherit quantum correlations directly from the reservoir without requiring an external laser pump. Owing to its robustness at high thermal occupancy ($n_{\text{th}} = 10^3$) and stability against variations in η and G, the system offers promising applications in quantum-enhanced metrology under elevated thermal conditions, simplified quantum communication networks with reduced size, weight, and power requirements, and robust entanglement distribution across noisy fiber-optic or satellite-to-ground links.

The vacuum state has the lowest possible energy in quantum optics; its quadrature fluctuations define the quantum "noise floor." To prove a light field is squeezed, one must show that in some quadrature the variance is below that of this vacuum benchmark only then is the field nonclassical. Especially for two modes, joint quadrature combinations (sums or differences) that beat vacuum variance are tied to entanglement via criteria like Duan or Simon. Normalizing this reduction yields a dimensionless squeezing measure for fair comparison across systems. Suppose $\hat{c}_\pm$ are Hermitian joint quadrature operators for a two-mode light field, with vacuum variances $\Delta c^2_{\pm,\text{vac}}$. Let the actual (steady-state or at time of interest) variance be $\Delta c^2_\pm$. From Two-mode light in optomechanical cavity with squeezed vacuum reservoirs [31] the degree of quadrature squeezing relative to vacuum as

$$S = \frac{\Delta c^2_{\pm,\text{vac}} - \Delta c^2_-}{\Delta c^2_{\pm,\text{vac}}} \tag{65}$$

where $\Delta c^2_{\pm,\text{vac}} = 2$ is quadrature variance of a two-mode vacuum state. If $S > 0$, there is squeezing; $S = 0$ means just vacuum level; $S < 0$ means noise above vacuum. Then according to Eq (63), Eq (65) written as:

$$S = -\Big[\Big(\langle \hat{a}_1^\dagger \hat{a}_1\rangle + \langle \hat{a}_2^\dagger \hat{a}_2\rangle\Big) - \Big(\langle \hat{a}_1^\dagger \hat{a}_2^\dagger\rangle + \langle \hat{a}_1 \hat{a}_2\rangle\Big)\Big] \tag{66}$$

$$\begin{aligned}
S = {} & \frac{4(\mu_4\mu_a + \mu_3\mu_b)|D_+|^4}{4\mu_a\mu_b|D_+|^4 + 2(\mu_a A_1^* + \mu_b A_1)|D_+|^2 + |A_1|^2 - 4\nu_3^2\nu_{13_-}^2(\mathrm{Re}D_+)^2} \\
& - \frac{\big(2(\mu_a A_3 + \mu_b A_2) - 2(\mu_4 A_1 + \mu_3 A_1^*) + 4\nu_3\nu_{13_-}(\mu_3 + \mu_4)\mathrm{Re}D_+\big)\,|D_+|^2}{4\mu_a\mu_b|D_+|^4 + 2(\mu_a A_1^* + \mu_b A_1)|D_+|^2 + |A_1|^2 - 4\nu_3^2\nu_{13_-}^2(\mathrm{Re}D_+)^2} \\
& + \frac{4\Big[D_+\big(\nu_3\mu_3\mu_b + \nu_{13_-}\mu_a\mu_4 - \nu_{13_+}\mu_a\mu_b\big) - D_+^*\big(\nu_{13_-}\mu_3\mu_b + \nu_3\mu_4\mu_a + \nu_3\mu_a\mu_b\big)\Big]|D_+|^2}{4\mu_a\mu_b|D_+|^4 + 2(\mu_a A_1^* + \mu_b A_1)|D_+|^2 + |A_1|^2 - 4\nu_3^2\nu_{13_-}^2(\mathrm{Re}D_+)^2} \\
& - \frac{(A_3A_1 + A_2A_1^*) - 2\nu_3\nu_{13_-}(A_2 + A_4)\mathrm{Re}D_+}{4\mu_a\mu_b|D_+|^4 + 2(\mu_a A_1^* + \mu_b A_1)|D_+|^2 + |A_1|^2 - 4\nu_3^2\nu_{13_-}^2(\mathrm{Re}D_+)^2} \\
& - \frac{2D_+^*\Big[\nu_{13_-}\mu_3 A_1^* + \nu_3\mu_4 A_1 + \nu_3\mu_a A_1^* + \nu_3\mu_b A_1\Big]}{4\mu_a\mu_b|D_+|^4 + 2(\mu_a A_1^* + \mu_b A_1)|D_+|^2 + |A_1|^2 - 4\nu_3^2\nu_{13_-}^2(\mathrm{Re}D_+)^2} \\
& + \frac{2D_+^*\Big[\nu_{13_-}\mu_b A_2 + \nu_3\mu_a A_3 + 2\nu_{13_-}\nu_3(\nu_{13_-}\mu_4 + \nu_3\mu_3)\mathrm{Re}D_+\Big]}{4\mu_a\mu_b|D_+|^4 + 2(\mu_a A_1^* + \mu_b A_1)|D_+|^2 + |A_1|^2 - 4\nu_3^2\nu_{13_-}^2(\mathrm{Re}D_+)^2} \\
& + \frac{2D_+\Big[\nu_3\mu_3 A_1^* + \nu_{13_-}\mu_4 A_1 - \nu_{13_+}\mu_a A_1^* - \nu_{13_+}\mu_b A_1\Big]}{4\mu_a\mu_b|D_+|^4 + 2(\mu_a A_1^* + \mu_b A_1)|D_+|^2 + |A_1|^2 - 4\nu_3^2\nu_{13_-}^2(\mathrm{Re}D_+)^2} \\
& - \frac{2D_+\Big[\nu_3\mu_b A_2 + \nu_{13_-}\mu_a A_3 + 2\nu_3\nu_{13_-}(\mu_4 + \mu_3)\mathrm{Re}D_+\Big]}{4\mu_a\mu_b|D_+|^4 + 2(\mu_a A_1^* + \mu_b A_1)|D_+|^2 + |A_1|^2 - 4\nu_3^2\nu_{13_-}^2(\mathrm{Re}D_+)^2}
\end{aligned}$$

$$+\frac{\nu_{13_-}A_2A_1^*+\nu_3A_3A_1-\nu_3|A_1|^2-2\nu_{13_-}\nu_3(\nu_{13_-}A_4+\nu_3A_2)\mathrm{Re}D_+ +4\nu_3^3\nu_{13_-}^2(\mathrm{Re}D_+)^2}{D_+\left(4\mu_a\mu_b|D_+|^4+2(\mu_aA_1^*+\mu_bA_1)|D_+|^2+|A_1|^2-4\nu_3^2\nu_{13_-}^2(\mathrm{Re}D_+)^2\right)}$$
$$-\frac{\nu_3A_2A_1^*+\nu_{13_-}A_3A_1+\nu_{13_+}|A_1|^2+2\nu_3^2\nu_{13_-}(A_4+A_2)\mathrm{Re}D_+ -4\nu_3^2\nu_{13_-}^2\nu_{13_+}(\mathrm{Re}D_+)^2}{D_+^*\left(4\mu_a\mu_b|D_+|^4+2(\mu_aA_1^*+\mu_bA_1)|D_+|^2+|A_1|^2-4\nu_3^2\nu_{13_-}^2(\mathrm{Re}D_+)^2\right)} \quad (67)$$

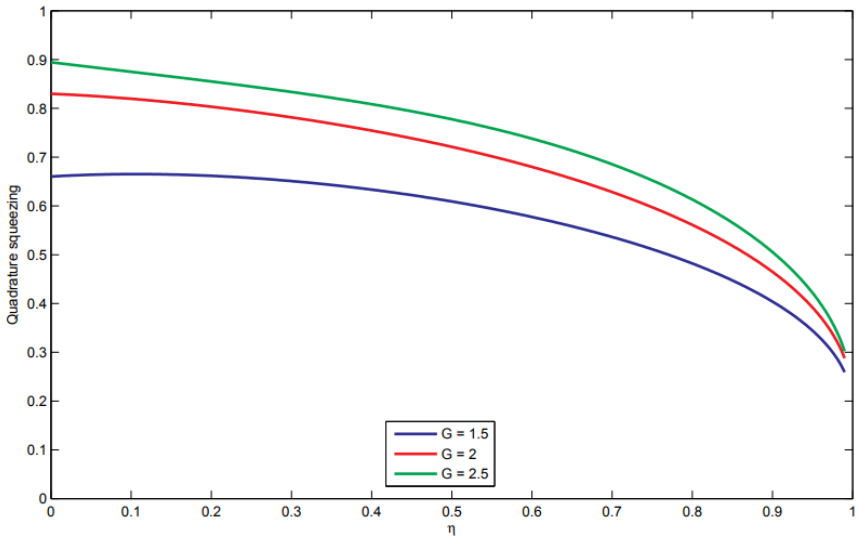

Figure 6. *Plots of S [Eq (67)] versus η for $\kappa = 0.8$, $r = 1.0$, $\gamma_c = 0.1$, $C_{0_1} = C_{0_2} = 10^{-2}$, $n_{th_1} = n_{th_2} = 10^2$, $\gamma = 0.1$; for different values of G.*

Figure 6 illustrates the S of a two-mode light system as a function of the parameter η, which represents an entanglement or correlation parameter related to the input states, for three different values of the G. The highest squeezing occurs at low values of η. At $\eta = 0$, the squeezing strength reaches approximately 65% to 90%, depending on the gain. Increasing the G significantly enhances the squeezing. This suggests that the amplification process helps overcome the high thermal noise ($n_{th} = 100$) specified in the parameters. The squeezing is caused by quantum correlations, represented by the $\langle \hat{a}_1 \hat{a}_2 \rangle$ terms in Eq. 66, between the two modes of light. These correlations are generated through interactions between photons and mechanical phonons, governed by the optomechanical cooperativity (C_0).

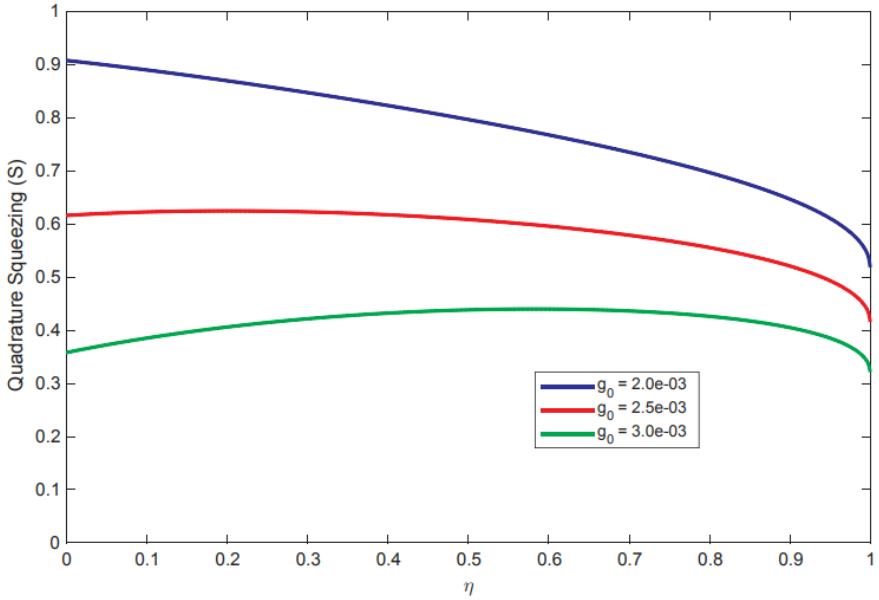

Figure 7. *Plots of S [Eq (67)] versus η for $\kappa = 0.8$, $r = 0.50$, $\gamma_c = \gamma_m = 0.1$, $G = 1$, $n_{th_1} = n_{th_2} = 10^3$, $\gamma = 0.1$; for different values of $g_{0_1} = g_{0_2} = g_0$.*

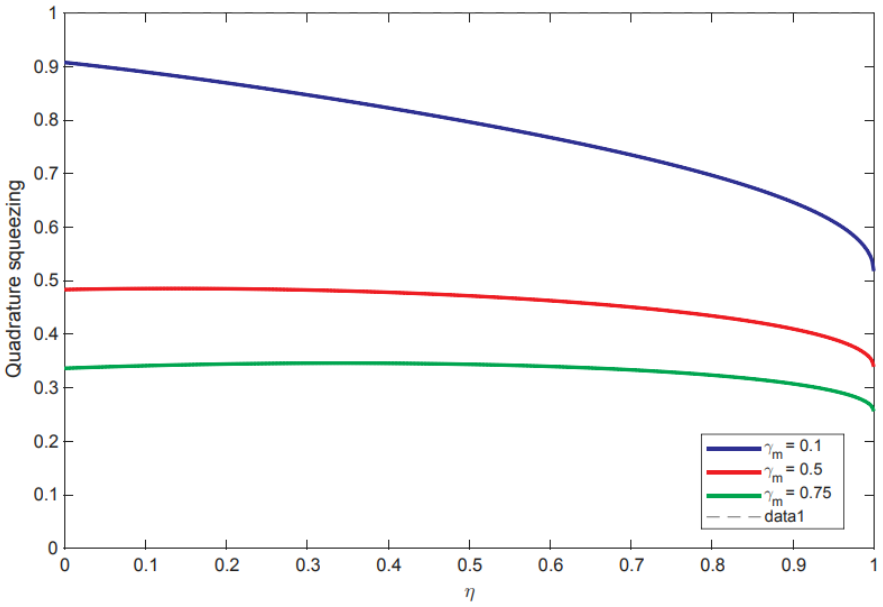

Figure 8. *Plots of S [Eq (67)] versus η for* $\kappa = 0.8$, $r = 0.50$,$g_{01} = g_{02} = 2e^{-3}$, $\gamma_c = 0.1$, $G = 1$, $n_{th_1} = n_{th_2} = 10^3$, $\gamma = 0.1$*; for different values of* γ_m.

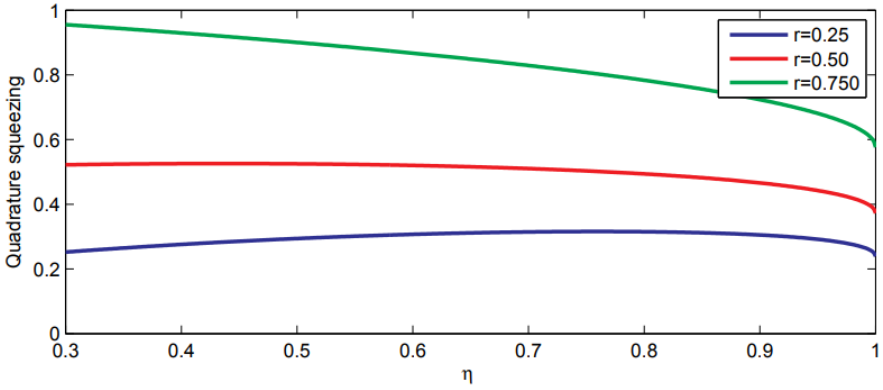

Figure 9. *Plots of S [Eq (67)] versus η for* $\kappa = 0.8$, $G = 1$, $\gamma_c = 0.1$, $C_{0_1} = C_{0_2} = 10^{-3}$, $n_{th_1} = n_{th_2} = 10^3$, $\gamma = 0.1$*; for different values of r.*

Figure 9, shows the quadrature squeezing for different reservoir squeezing parameters. For the blue solid curve (r = 0.25), corresponding to weak reservoir squeezing, the squeezing increases with η, reaches a shallow maximum, and slightly decreases as $\eta \to 1$, remaining relatively weak overall. For the red solid curve (r = 0.50), the squeezing is significantly enhanced across the entire range of η, exhibiting a broad maximum due to the cooperative effect of atomic coherence and reservoir squeezing. The green solid curve (r = 0.75) shows the strongest squeezing, with a substantial reduction of the quadrature variance for all η. Although a slight degradation occurs as $\eta \to 1$, pronounced squeezing persists throughout.
In Figure 6 as G increases from 1.5 to 2.5, the squeezing S increases significantly, reaching approximately 90% at low η. While the reservoir provides the seed for correlations, the gain G acts as an amplifier, enabling the quantum signal to overcome the substantial thermal noise floor ($n_{\text{th}} = 10^2$ to 10^3). Figure 4 ($r = 1.0$) exhibits deeper squeezing in the variance Δc_-^2 than Figure 5 ($r = 0.25$), and Figure 9 similarly shows S increasing sharply with r, confirming that the reservoir serves as the primary driving mechanism of the system. In the absence of a coherent pump, the system relies entirely on the squeeze parameter r to establish entanglement between the modes. Figure 7 shows that increasing the single-photon coupling g_0 from 2.0×10^{-3} to 3.0×10^{-3} enhances squeezing, while Figure 8 demonstrates that lower mechanical decay ($\gamma_m = 0.1$) yields stronger squeezing. Higher cooperativity (C_0) and reduced damping allow the quantum correlations injected by the reservoir to persist longer before dissipating into the environment. The most significant aspect of this research is its broad operational range, as externally injected reservoir correlations produce squeezing largely independent of η, thereby enhancing experimental feasibility without requiring precise operating conditions. Sustaining squeezing at $n_{\text{th}} = 1000$ without a high-power pump, it enables robust, low-energy, cryogen-free quantum technologies.

3.2. Entanglement Properties of the Two-Mode Cavity

In this section, we would like to investigate the entanglement properties of the two-mode light. In general a quantum state of system ρ of two-modes a_1 and a_2 is said to be disentangled iff

$$\hat{\rho} = \sum_j P_j \hat{\rho}_j^{(a_1)} \otimes \hat{\rho}_j^{(a_2)}, \tag{68}$$

where $\rho_j^{(a_1)}$ and $\rho_j^{(a_2)}$ are assumed to be the normalized density operator of mode a_1 and a_2, respectively $P_j \geq 0$ and $\sum_j P_j = 1$. Otherwise it is said to be entangled. Entanglement criteria for continuous variables which are based on the inseparability of the system density matrix. In this paper we apply one of these criteria in order to verify the entanglement between the two modes in the cavity. A quantum state of a system is said to be entangled if the sum of the variances of the EPR-like quadrature operators, $\hat{u}$ and $\hat{v}$, satisfy the inequality

$$\Delta u^2 + \Delta v^2 < 2, \tag{69}$$

where u and v are pair of EPR-type continues variables defined by

$$\hat{u} = \hat{x}_1 - \hat{x}_2, \quad \hat{v} = \hat{p}_1 + \hat{p}_2, \tag{70}$$

with

$$\hat{x}_1 = \frac{1}{\sqrt{2}}\left(\hat{a}_1^\dagger + \hat{a}_1\right), \quad \hat{x}_2 = \frac{1}{\sqrt{2}}\left(\hat{a}_2^\dagger + \hat{a}_2\right), \tag{71}$$

$$\hat{p}_1 = \frac{i}{\sqrt{2}}\left(\hat{a}_1^\dagger - \hat{a}_1\right), \quad \hat{p}_2 = \frac{i}{\sqrt{2}}\left(\hat{a}_2^\dagger - \hat{a}_2\right). \tag{72}$$

The total variance of these two variables reduces to zero for maximally entangled continuous variable states. We next proceed to calculate the variance of EPR-type operators. To this end, using Eqs. (70) - (72), the variance of EPR-type variables defined by

$$\begin{aligned} \Delta u^2 &= \langle \hat{u}^2 \rangle - \langle \hat{u} \rangle^2 = \langle \hat{u}, \hat{u} \rangle, \\ \Delta v^2 &= \langle \hat{v}^2 \rangle - \langle \hat{v} \rangle^2 = \langle \hat{v}, \hat{v} \rangle, \end{aligned} \tag{73}$$

Because of $\langle \hat{v} \rangle^2 = \langle \hat{u} \rangle^2 = 0$, by taking Eq. (70)in account Eqs. (69) yields

$$\Delta u^2 + \Delta v^2 = \langle \hat{u}, \hat{u} \rangle + \langle \hat{v}, \hat{v} \rangle \tag{74}$$

From Eqs. (71) and Eqs. (72)

$$\begin{aligned} \hat{u} &= \hat{x}_1 - \hat{x}_2 = \frac{1}{\sqrt{2}}\left(\hat{a}_1^\dagger + \hat{a}_1 - \hat{a}_2^\dagger - \hat{a}_2\right) \\ \hat{v} &= \hat{p}_1 + \hat{p}_2 = \frac{i}{\sqrt{2}}\left(\hat{a}_1^\dagger - \hat{a}_1 + \hat{a}_2^\dagger - \hat{a}_2\right) \end{aligned} \tag{75}$$

Therefore

$$\hat{u}^2 + \hat{v}^2 = 2(\hat{a}_1 - \hat{a}_2^\dagger)(\hat{a}_1^\dagger - \hat{a}_2) \tag{76}$$

With the bosonic commutation relations of Eqs. (76), expanding in to convenient normally-ordered form is

$$\hat{u}^2 + \hat{v}^2 = 2\left(\hat{a}_1^\dagger \hat{a}_1 + \hat{a}_2^\dagger \hat{a}_2 - \hat{a}_1 \hat{a}_2 - \hat{a}_1^\dagger \hat{a}_2^\dagger\right) + 2 \tag{77}$$

Since $\hat{a}_i \hat{a}_i^\dagger = \hat{a}_i^\dagger \hat{a}_i + 1$. Therefore for the variances for $\langle \hat{u} \rangle^2 = \langle \hat{v} \rangle^2 = 0$ becomes

$$\begin{aligned} &\Delta u^2 + \Delta v^2 = \\ &2 + 2\Big[\langle \hat{a}_1^\dagger \hat{a}_1 \rangle + \langle \hat{a}_2^\dagger \hat{a}_2 \rangle - (\langle \hat{a}_1 \hat{a}_2 \rangle + \langle \hat{a}_1^\dagger \hat{a}_2^\dagger \rangle)\Big] \end{aligned} \tag{78}$$

$$\begin{aligned} \Delta u^2 + \Delta v^2 = 2 &- \frac{8(\mu_4\mu_a + \mu_3\mu_b)|D_+|^4}{4\mu_a\mu_b|D_+|^4 + 2(\mu_a A_1^* + \mu_b A_1)|D_+|^2 + |A_1|^2 - 4\nu_3^2\nu_{13_-}^2(\mathrm{Re}D_+)^2} \\ &+ \frac{2\left(2(\mu_a A_3 + \mu_b A_2) - 2(\mu_4 A_1 + \mu_3 A_1^*) + 4\nu_3\nu_{13_-}(\mu_3 + \mu_4)\mathrm{Re}D_+\right)|D_+|^2}{4\mu_a\mu_b|D_+|^4 + 2(\mu_a A_1^* + \mu_b A_1)|D_+|^2 + |A_1|^2 - 4\nu_3^2\nu_{13_-}^2(\mathrm{Re}D_+)^2} \\ &- \frac{8\Big[D_+\left(\nu_3\mu_3\mu_b + \nu_{13_-}\mu_a\mu_4 - \nu_{13_+}\mu_a\mu_b\right) - D_+^*\left(\nu_{13_-}\mu_3\mu_b + \nu_3\mu_4\mu_a + \nu_3\mu_a\mu_b\right)\Big]|D_+|^2}{4\mu_a\mu_b|D_+|^4 + 2(\mu_a A_1^* + \mu_b A_1)|D_+|^2 + |A_1|^2 - 4\nu_3^2\nu_{13_-}^2(\mathrm{Re}D_+)^2} \\ &+ \frac{2\left((A_3A_1 + A_2A_1^*) - 2\nu_3\nu_{13_-}(A_2 + A_4)\mathrm{Re}D_+\right)}{4\mu_a\mu_b|D_+|^4 + 2(\mu_a A_1^* + \mu_b A_1)|D_+|^2 + |A_1|^2 - 4\nu_3^2\nu_{13_-}^2(\mathrm{Re}D_+)^2} \\ &+ \frac{4D_+^*\Big[\nu_{13_-}\mu_3 A_1^* + \nu_3\mu_4 A_1 + \nu_3\mu_a A_1^* + \nu_3\mu_b A_1\Big]}{4\mu_a\mu_b|D_+|^4 + 2(\mu_a A_1^* + \mu_b A_1)|D_+|^2 + |A_1|^2 - 4\nu_3^2\nu_{13_-}^2(\mathrm{Re}D_+)^2} \\ &- \frac{4D_+^*\Big[\nu_{13_-}\mu_b A_2 + \nu_3\mu_a A_3 + 2\nu_{13_-}\nu_3(\nu_{13_-}\mu_4 + \nu_3\mu_3)\mathrm{Re}D_+\Big]}{4\mu_a\mu_b|D_+|^4 + 2(\mu_a A_1^* + \mu_b A_1)|D_+|^2 + |A_1|^2 - 4\nu_3^2\nu_{13_-}^2(\mathrm{Re}D_+)^2} \\ &- \frac{4D_+\Big[\nu_3\mu_3 A_1^* + \nu_{13_-}\mu_4 A_1 - \nu_{13_+}\mu_a A_1^* - \nu_{13_+}\mu_b A_1\Big]}{4\mu_a\mu_b|D_+|^4 + 2(\mu_a A_1^* + \mu_b A_1)|D_+|^2 + |A_1|^2 - 4\nu_3^2\nu_{13_-}^2(\mathrm{Re}D_+)^2} \end{aligned}$$

$$+\frac{4D_{+}\left[\nu_{3}\mu_{b}A_{2}+\nu_{13_{-}}\mu_{a}A_{3}+2\nu_{3}\nu_{13_{-}}(\mu_{4}+\mu_{3})\mathrm{Re}D_{+}\right]}{4\mu_{a}\mu_{b}|D_{+}|^{4}+2(\mu_{a}A_{1}^{*}+\mu_{b}A_{1})|D_{+}|^{2}+|A_{1}|^{2}-4\nu_{3}^{2}\nu_{13_{-}}^{2}(\mathrm{Re}D_{+})^{2}}$$
$$-\frac{2\left(\nu_{13_{-}}A_{2}A_{1}^{*}+\nu_{3}A_{3}A_{1}-\nu_{3}|A_{1}|^{2}-2\nu_{13_{-}}\nu_{3}(\nu_{13_{-}}A_{4}+\nu_{3}A_{2})\mathrm{Re}D_{+}+4\nu_{3}^{3}\nu_{13_{-}}^{2}(\mathrm{Re}D_{+})^{2}\right)}{D_{+}\left(4\mu_{a}\mu_{b}|D_{+}|^{4}+2(\mu_{a}A_{1}^{*}+\mu_{b}A_{1})|D_{+}|^{2}+|A_{1}|^{2}-4\nu_{3}^{2}\nu_{13_{-}}^{2}(\mathrm{Re}D_{+})^{2}\right)}$$
$$+\frac{2\left(\nu_{3}A_{2}A_{1}^{*}+\nu_{13_{-}}A_{3}A_{1}+\nu_{13_{+}}|A_{1}|^{2}+2\nu_{3}^{2}\nu_{13_{-}}(A_{4}+A_{2})\mathrm{Re}D_{+}-4\nu_{3}^{2}\nu_{13_{-}}^{2}\nu_{13_{+}}(\mathrm{Re}D_{+})^{2}\right)}{D_{+}^{*}\left(4\mu_{a}\mu_{b}|D_{+}|^{4}+2(\mu_{a}A_{1}^{*}+\mu_{b}A_{1})|D_{+}|^{2}+|A_{1}|^{2}-4\nu_{3}^{2}\nu_{13_{-}}^{2}(\mathrm{Re}D_{+})^{2}\right)} \tag{79}$$

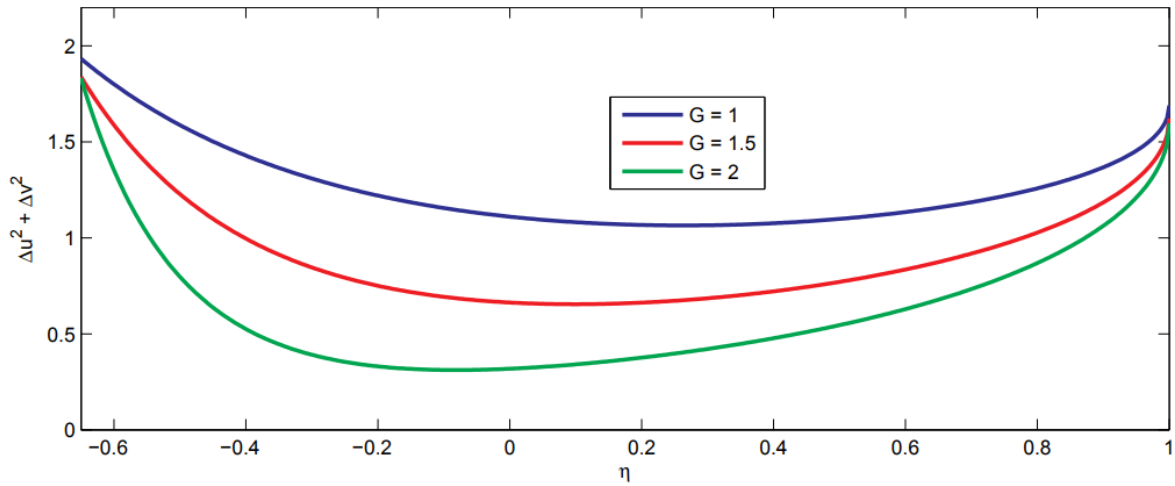

Figure 10. *Plots of $\Delta u^2+\Delta v^2$ [Eq (79)] versus η for $\kappa=0.8$, $r=1.0$, $\gamma=0.1$, $\gamma_c=0.1$,$n_{th_1}=n_{th_2}=1e^3$, $C0_1=C0_2=1e^-3$; and for different values of G.*

Figure 10 shows the dependence of the summed variances of the EPR-like quadrature operators, $\Delta u^2+\Delta v^2$, on the parameter η for three values of the gain (or coupling) parameter G. For $G=1$, the variance sum remains close to unity and below the separability bound of 2, indicating moderate entanglement. Increasing the gain to $G=1.5$ and $G=2$ results in progressively lower minima of the variance sum, reflecting enhanced entanglement. In all cases, the entanglement criterion $\Delta u^2+\Delta v^2<2$ is satisfied over the considered range of η. The minimum variance occurs at an optimal value of η (approximately 0-0.2), and the degree of entanglement increases monotonically with G.

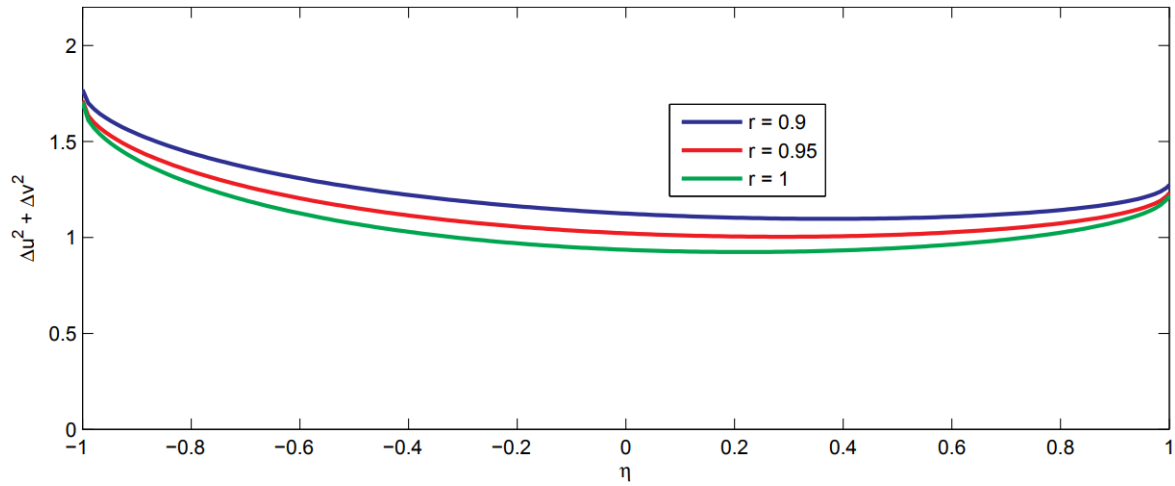

Figure 11. *Plots of $\Delta u^2+\Delta v^2$ [Eq (79)] versus η for $\kappa=0.8$, $G=0.50$, $\gamma=0.1$, $\gamma_c=0.1$, $n_{th_1}=n_{th_2}=1.55e^3$, $C0_1=C0_2=0.5e^-3$; and for different values of r.*

The Figure 11 examines the entanglement of a two-mode quantum system using the DGCZ inseparability criterion, which identifies entanglement when $\Delta u^2 + \Delta v^2 < 2$. The Figure 11 shows the dependence of the variance sum on the population inversion parameter η and the squeezing parameter r, demonstrating that higher pumping rates and stronger population inversion enhance entanglement. Notably, entanglement persists despite significant thermal noise (n_{th}), facilitated by low linear gain (G) and cooperativity (C_0). These results highlight the relevance of the system for continuous-variable quantum information applications.

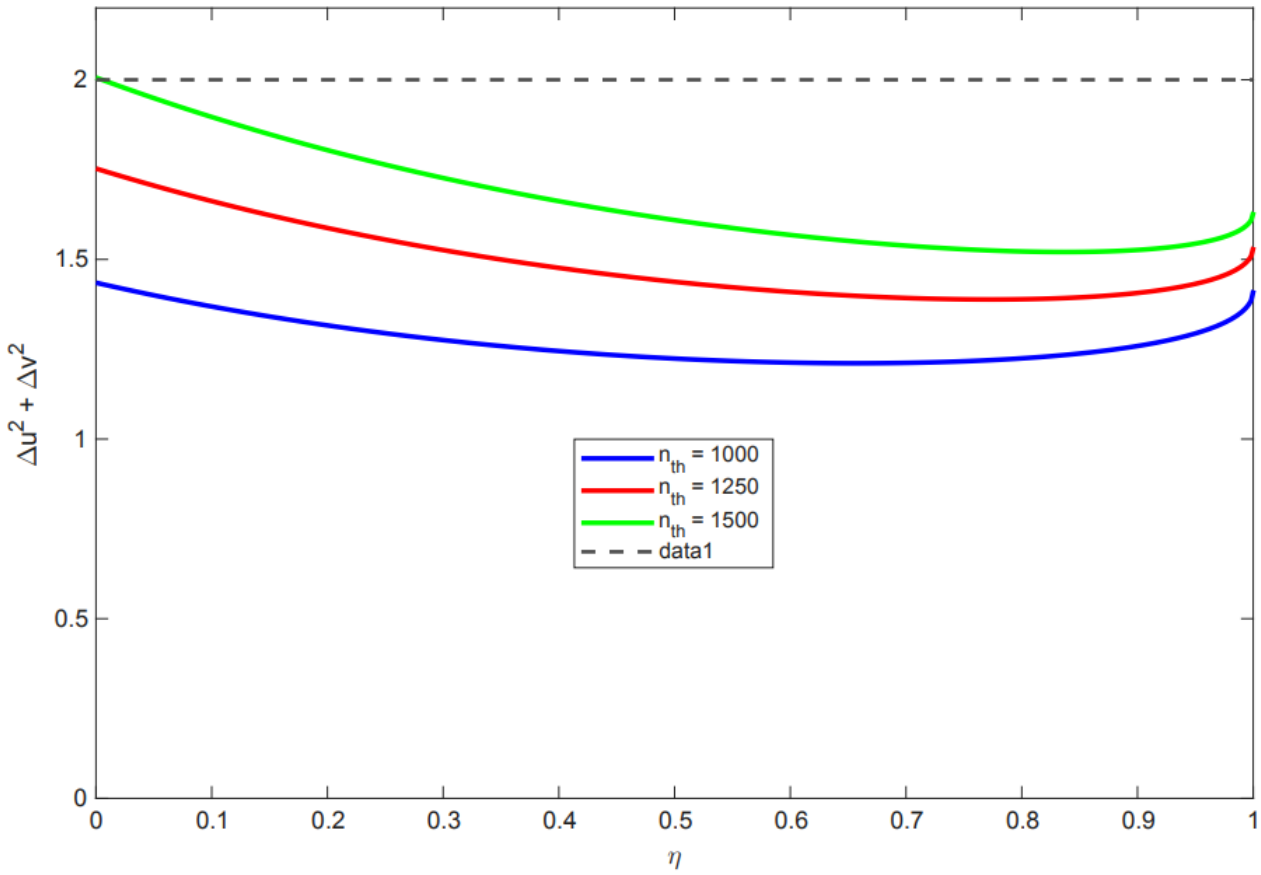

Figure 12. *Plots of $\Delta u^2 + \Delta v^2$ [Eq (79)] versus η for $\kappa = 0.8$, $G = 1$, $\gamma = 0.1$, $r = 0.5$ $\gamma_c = 0.1$, $C0_1 = C0_2 = 0.5e^-3$; and for different values of $n_{th_1} = n_{th_2}$.*

Figure 12 illustrates the variance sum $\Delta u^2 + \Delta v^2$ as a function of the population inversion parameter η for varying thermal phonon occupations ($n_{\text{th}} = 1000, 1250, 1500$). The findings show that, even at very high thermal occupations ($n_{\text{th}} = 1500$), the curves remain entirely below the vacuum threshold (the dashed line at 2), indicating the presence of robust entanglement. As n_{th} increases, the variance sum rises (approaching 2), which arises from the increased noise contribution in the $\langle \hat{a}_i^\dagger \hat{a}_i \rangle$ terms. However, the system's ability to remain below 2 at such elevated values constitutes a significant result. Unlike conventional optomechanical systems that rely on strong coherent lasers, this setup uses correlations injected by a squeezed vacuum reservoir to passively entangle atoms and mechanical modes, robustly stabilizing quantum correlations and protecting entanglement against thermal decoherence for practical continuous-variable quantum information applications. Because the findings demonstrate entanglement at $n_{\text{th}} = 1500$, the results suggest a pathway toward quantum technologies capable of operating in noisy or non-cryogenic environments.

4. Conclusion

This investigation establishes that a hybrid atom-optomechanical system can achieve robust, steady-state quantum correlations induced solely by a squeezed vacuum reservoir, eliminating the requirement for external coherent driving. By harnessing the reservoir as a pre-correlated environment, the architecture demonstrates remarkable resilience to thermal decoherence, preserving multipartite entanglement and quadrature squeezing even at thermal phonon occupations as high as $n_{\text{th}} = 1500$. Unlike traditional models that require precise population inversion or high-power pumps to overcome noise, this pump-free approach offers broad operational stability. It also facilitates experimental realization through its independence from

stringent gain and coupling constraints. The redistribution of quantum noise within the Heisenberg uncertainty limits, facilitated by optomechanical cooperativity, ensures that the system maintains high-fidelity squeezing across a wide parameter space. Ultimately, these findings suggest a transformative pathway for quantum-enhanced metrology, secure communication, and robust entanglement distribution in realistic, cryogen-free environments where size, weight, and power efficiency are paramount.

ORCID

0009-0003-2979-2400 (Adagn Addisu Dabulo)

Abbreviations

DGCZ	Duan-Giedke-Cirac-Zoller
CQED	Cavity Quantum Electrodynamics
S	Quadrature Squeezing
G	Linear Gain Coefficient

Author Contributions

Adagn Addisu Dabulo: Formal Analysis, Funding acquisition, Investigation, Methodology, Resources, Software, Supervision, Validation, Visualization, Writing original draft, Writing - review & editing

Data Availability Statement

No data sets were generated or analyzed during the current study. All relevant information supporting the findings of this study is included within the article.

Conflicts of Interests

The authors declare no conflicts of interest.

Appendix

Thermal Phonon Occupation n_{th}.

$$n_{\text{th}} = \frac{1}{e^{\hbar\omega_m/k_BT} - 1} \tag{80}$$

Linear Gain Coefficient G.

$$G = \frac{2g^2 r_1}{\gamma^2} \tag{81}$$

Single-Photon Optomechanical Cooperativity C_0.

$$C_{0_i} = \frac{4g_{0_i}^2}{\kappa\gamma_m} \tag{82}$$

Table 1. *Minimum and maximum experimentally reported parameter ranges for NASA-affiliated hybrid atom–optomechanical systems.*

Parameter	Minimum	Maximum
$\frac{g_{0m}}{2\pi}$	0.10 Hz	1.0 MHz
$\frac{\kappa}{2\pi}$	0.1 kHz	10 MHz
$\frac{\omega_m}{2\pi}$	10 Hz	100 MHz
Q_m	10^4	10^9
n_{th}	10^2	10^6
C_0	10^{-3}	10^6
T	$10\ m\ K$	$20\ m\ K$

These values are inferred from lasing thresholds, gain narrowing, and noise spectra in NASA-funded cavity-QED experiments [34–36].
Thus mechanical damping:

$$\gamma_m = \frac{\omega_m}{Q_m} \tag{83}$$

Linear gain coefficient:

$$G = \frac{2g^2 r_a}{\gamma^2} \tag{84}$$

Stimulated emission decay constant:

$$\gamma_c = \frac{4g^2}{\kappa} \tag{85}$$

Initial populations for cascade levels (1 = upper, 2 = middle, 3 = lower):

$$\rho_{11}^{(0)} = \frac{1-\eta}{2}, \quad \rho_{33}^{(0)} = \frac{1+\eta}{2} \tag{86}$$

where $\eta \in [-1, 1]$ is the population inversion parameter and relating G and γ_c;

$$G = \frac{\kappa r_a}{2\gamma^2}\gamma_c \tag{87}$$

This is a direct linear relation between G and γ_c.
For a three-level cascade system $|1\rangle \rightarrow |2\rangle \rightarrow |3\rangle$, only the population in the upper level contributes to stimulated emission into the cavity mode and the effective atomic injection rate:

$$r_a = R\rho_{11}^{(0)} = R\frac{1-\eta}{2} \tag{88}$$

where R is the atomic flux through the cavity, substituting into previous equation

$$G = \frac{\kappa R}{4\gamma^2}(1-\eta)\gamma_c \tag{89}$$

This expresses linear gain in terms of stimulated emission decay, cavity losses, atomic inversion, and atomic flux.

Definitions:

$$\mu_1 = \tfrac{1}{2}\Big(\kappa(N+1) + \frac{\gamma\kappa}{2\gamma_c}\Big), \quad \mu_3 = \tfrac{1}{2}\big(\kappa N + G\rho_{11}^{(0)}\big), \quad \mu_2 = \tfrac{1}{2}\Big(\kappa(N+1) + \frac{\gamma\kappa}{2\gamma_c} + G\rho_{33}^{(0)}\Big), \quad \mu_4 = \tfrac{\kappa N}{2}$$
$$\nu_1 = \kappa M_a, \quad \nu_2 = \frac{G\rho_{13}^{(0)}}{2} + \kappa M_a = \frac{G\rho_{13}^{(0)}}{2} + \nu_1, \quad \nu_3 = \frac{G\rho_{31}^{(0)}}{2} + \kappa M_a = \frac{G\rho_{31}^{(0)}}{2} + \nu_1$$
$$N_1 = \tfrac{C_{0_1}\kappa}{2} - \mu_1, \quad N_2 = \tfrac{C_{0_1}\kappa}{2} + \mu_1, \quad M_1 = \tfrac{C_{0_2}\kappa}{2} - \mu_2, \quad M_2 = \tfrac{C_{0_2}\kappa}{2} + \mu_2$$
$$T_1 = C_{0_1}\kappa(n_{th,1}+1), \quad T_2 = C_{0_1}\kappa n_{th,1}, \quad T_3 = C_{0_2}\kappa(n_{th,2}+1), \quad T_4 = C_{0_2}\kappa n_{th,2} \tag{90}$$

Let define additional constants

$$\mu_a = \mu_3 - \mu_1, \quad \mu_b = \mu_4 - \mu_2, \quad \mu_a + \mu_b = \mu_4 + \mu_3 - \mu_1 - \mu_2, \quad X_+ = X_1 + X_2$$
$$\nu_a = T_1 + T_2 = C_{0_1}\kappa(2n_{th,1}+1), \quad \nu_b = T_3 + T_4 = C_{0_2}\kappa(2n_{th,2}+1), \quad X_- = X_2 - X_1$$
$$\sum_{j=1}^{4} T_j = \nu_a + \nu_b, \quad \rho_{11}^{(0)} = \frac{1-\eta}{2}, \quad \rho_{33}^{(0)} = \frac{1+\eta}{2}, \quad \rho_{33}^{(0)} - \rho_{11}^{(0)} = \eta, \quad \rho_{11}^{(0)} - \rho_{33}^{(0)} = -\eta,$$
$$\rho_{13}^{(0)} = \rho_{31}^{(0)} = \frac{\sqrt{1-\eta^2}}{2}, \quad \rho_{11}^{(0)} + \rho_{33}^{(0)} = 1, \quad \rho_{13}^{(0)} + \rho_{31}^{(0)} = \sqrt{1-\eta^2}, \quad \rho_{13}^{(0)}\big(\rho_{13}^{(0)} + \rho_{31}^{(0)}\big) = \frac{1-\eta^2}{2} \tag{91}$$

Define

$$\mu_{12} = \mu_1 + \mu_2, \quad \mu_{34} = \mu_3 + \mu_4 \tag{92}$$

Define other alternative constants as:

$$C_1 = D_1 D_{+c} + \nu_2\nu_3, \quad C_2 = D_2 D_- + (\nu_1 - \nu_2)(\nu_1 - \nu_3), \quad D_1 = \mu_a + iX_1 - 2\nu_a, \quad D_1^* = \mu_a - iX_1 - 2\nu_a$$
$$D_2 = \mu_b + iX_2 - 2\nu_b, \quad D_2^* = \mu_b - iX_2 - 2\nu_b, \quad D_- = \mu_a + \mu_b + iX_- - \nu a - \nu_b, \quad D{+}c = \mu_a + \mu_b - iX_- - \nu_a - \nu_b$$
$$D_+ = \mu_a + \mu_b + iX_+ - \nu_a - \nu_b, \quad K_1 = \frac{\nu_2 + \nu_3 - \nu_1}{2\mu_a}, \quad K_2 = \frac{\nu_1 - \nu_2 - \nu_3}{2\mu_b}$$
$$D_3 = \mu_{12} - iX_- + \nu_a + \nu_b, \quad \nu_{12_+} = \nu_1 + \nu_2$$
$$\nu_{12_-} = \nu_1 - \nu_2, \quad \nu_{13_+} = \nu_1 + \nu_3, \quad \nu_{13_-} = \nu_1 - \nu_3, \quad \nu_{ab_+} = \nu_a + \nu_b$$
$$D_+^* = \mu_a + \mu_b - iX_+ - \nu_a - \nu_b, D_3^* = \mu_{12} + iX_- + \nu_a + \nu_b \tag{93}$$

Let define:

$$A_3 = -\nu_{12_-}\nu_{13_+}D_+ - \nu_3\nu_2 D_+^*, \quad A_1 = \nu_2\nu_3 D_+ + \nu_{13_-}\nu_{12_-}D_+^*, \quad A_1^* = \nu_2\nu_3 D_+^* + \nu_{13_-}\nu_{12_-}D_+$$
$$2ReD_+ = (D_+ + D_+^*), \quad A_2 = -\nu_2\nu_{13_+}D_+ + \nu_2\nu_{13_-}D_+^*, \quad A_4 = -\nu_{12_-}\nu_{13_+}D_+ - \nu_3\nu_2 D_+^* \tag{94}$$
$$|A_1|^2 = \left[\kappa^4 M_a^4 + G\kappa^3 M_a^3\sqrt{1-\eta^2} + \frac{3G^2\kappa^2 M_a^2}{8}(1-\eta^2) + \frac{G^3\kappa M_a}{32}(1-\eta^2)^{3/2} + \frac{G^4}{128}(1-\eta^2)^2\right]|D_+|^2$$
$$+\left[\frac{G^2\kappa^2 M_a^2}{8}(1-\eta^2) + \frac{G^3\kappa M_a}{16}(1-\eta^2)^{3/2} + \frac{G^4}{128}(1-\eta^2)^2\right](\mathrm{Re}D_+)^2 \tag{95}$$

$$D_1 = \frac{G}{4}(1-\eta) - \kappa\left(\frac{1}{2} + \frac{\gamma}{4\gamma_c} + \frac{3}{2}C_{0_1} + 4C_{0_1}n_{\mathrm{th},1}\right)$$
$$D_1^* = \frac{G}{4}(1-\eta) - \kappa\left(\frac{1}{2} + \frac{\gamma}{4\gamma_c} + \frac{5}{2}C_{0_1} + 4C_{0_1}n_{\mathrm{th},1}\right) \tag{96}$$

$$D_2 = -\frac{G}{4}(1+\eta) - \kappa\left[\frac{1}{2} + \frac{\gamma}{4\gamma_c} + C_{0_2}\left(4n_{\mathrm{th},2} + \frac{3}{2}\right)\right]$$
$$D_2^* = -\frac{G}{4}(1+\eta) - \kappa\left[\frac{1}{2} + \frac{\gamma}{4\gamma_c} + C_{0_2}\left(4n_{\mathrm{th},2} + \frac{5}{2}\right)\right] \tag{97}$$

$$D_3 = \frac{G}{4}(1+\eta) + \kappa\Big[(N+1) + \frac{\gamma}{2\gamma_c} + C_{0_1}(2n_{\mathrm{th},1} + \tfrac{3}{2}) + C_{0_2}(2n_{\mathrm{th},2} + \tfrac{1}{2})\Big]$$
$$D_3^* = \frac{G}{4}(1+\eta) + \kappa\Big[(N+1) + \frac{\gamma}{2\gamma_c} + C_{0_1}(2n_{\mathrm{th},1} + \tfrac{1}{2}) + C_{0_2}(2n_{\mathrm{th},2} + \tfrac{3}{2})\Big] \tag{98}$$

$$D_+^* = -\frac{G\eta}{2} - \kappa\left[1 + \frac{\gamma}{2\gamma_c} + C_{0_1}\Big(2n_{\mathrm{th},1} + \tfrac{3}{2}\Big) + C_{0_2}\Big(2n_{\mathrm{th},2} + \tfrac{3}{2}\Big)\right]$$
$$D_+ = -\frac{G\eta}{2} - \kappa\left[1 + \frac{\gamma}{2\gamma_c} + C_{0_1}\Big(2n_{\mathrm{th},1} + \tfrac{1}{2}\Big) + C_{0_2}\Big(2n_{\mathrm{th},2} + \tfrac{1}{2}\Big)\right] \tag{99}$$

$$\mathrm{Re}D_+ = -\frac{G\eta}{2} - \kappa - \frac{\gamma\kappa}{2\gamma_c} - \kappa\Big[C_{0_1}(2n_{\mathrm{th},1}+1) + C_{0_2}(2n_{\mathrm{th},2}+1)\Big]$$
$$D_+^* = -\frac{G\eta}{2} - \kappa - \frac{\gamma\kappa}{2\gamma_c} - \kappa\Big[C_{0_1}\big(2n_{\mathrm{th},1} + \tfrac{3}{2}\big) + C_{0_2}\big(2n_{\mathrm{th},2} + \tfrac{3}{2}\big)\Big] \tag{100}$$

$$A_3 = \kappa(C_{0_1} + C_{0_2})\left(\frac{G\kappa M_a}{2}\sqrt{1-\eta^2} + \frac{G^2}{16}(1-\eta^2)\right) - (\kappa M_a)^2 D_+^* \tag{101}$$

$$A_1 = -\kappa\left[\left(\kappa M_a + \frac{G}{4}\sqrt{1-\eta^2}\right)^2 + \frac{G^2}{16}(1-\eta^2)\right]\left(1 + \frac{\gamma}{2\gamma_c} + C_{0_1}(2n_{\mathrm{th},1} + \frac{1}{2}) + C_{0_2}(2n_{\mathrm{th},2} + \frac{1}{2})\right)$$
$$-\frac{G\eta}{2}\left[\left(\kappa M_a + \frac{G}{4}\sqrt{1-\eta^2}\right)^2 + \frac{G^2}{16}(1-\eta^2)\right] \tag{102}$$

$$A_1^* = -\kappa\left[\left(\kappa M_a + \frac{G}{4}\sqrt{1-\eta^2}\right)^2 + \frac{G^2}{16}(1-\eta^2)\right]\left(1 + \frac{\gamma}{2\gamma_c} + C_{0_1}(2n_{\mathrm{th},1} + \frac{3}{2}) + C_{0_2}(2n_{\mathrm{th},2} + \frac{3}{2})\right)$$
$$-\frac{G\eta}{2}\left[\left(\kappa M_a + \frac{G}{4}\sqrt{1-\eta^2}\right)^2 + \frac{G^2}{16}(1-\eta^2)\right] \tag{103}$$

$$A_2 = \left[2(\kappa M_a)^2 + \frac{3G}{4}\kappa M_a\sqrt{1-\eta^2} + \frac{G^2}{16}(1-\eta^2)\right]\left(\frac{G\eta}{2} + \kappa + \frac{\gamma\kappa}{2\gamma_c}\right)$$
$$+2\kappa\left[2(\kappa M_a)^2 + \frac{3G}{4}\kappa M_a\sqrt{1-\eta^2} + \frac{G^2}{16}(1-\eta^2)\right](C_{0_1}n_{\mathrm{th},1} + C_{0_2}n_{\mathrm{th},2})$$
$$+\frac{\kappa}{2}\left[2(\kappa M_a)^2 + \frac{3G}{4}\kappa M_a\sqrt{1-\eta^2} + \frac{G^2}{8}(1-\eta^2)\right](C_{0_1} + C_{0_2}) \tag{104}$$

$$A_4 = \left[(\kappa M_a)^2 + G\kappa M_a\sqrt{1-\eta^2} + \frac{G^2}{8}(1-\eta^2)\right]\left(\frac{G\eta}{2} + \kappa + \frac{\gamma\kappa}{2\gamma_c}\right)$$
$$+2\kappa\left[(\kappa M_a)^2 + G\kappa M_a\sqrt{1-\eta^2} + \frac{G^2}{8}(1-\eta^2)\right](C_{0_1}n_{\mathrm{th},1} + C_{0_2}n_{\mathrm{th},2})$$
$$+\frac{\kappa}{2}\left[3(\kappa M_a)^2 + 2G\kappa M_a\sqrt{1-\eta^2} + \frac{G^2}{8}(1-\eta^2)\right](C_{0_1} + C_{0_2}) \tag{105}$$

$$|D_+|^2 = \left(\frac{G\eta}{2} + \kappa + \frac{\gamma\kappa}{2\gamma_c} + 2\kappa(C_{0_1}n_{\mathrm{th},1} + C_{0_2}n_{\mathrm{th},2})\right)^2 + \frac{3\kappa^2}{4}(C_{0_1} + C_{0_2})^2$$
$$+2\kappa(C_{0_1} + C_{0_2})\left(\frac{G\eta}{2} + \kappa + \frac{\gamma\kappa}{2\gamma_c} + 2\kappa(C_{0_1}n_{\mathrm{th},1} + C_{0_2}n_{\mathrm{th},2})\right) \tag{106}$$

$$\mu_1 = \tfrac{1}{2}\Big(\kappa(N+1) + \frac{\gamma\kappa}{2\gamma_c}\Big), \quad \mu_3 = \frac{\kappa N}{2} + \frac{G}{4}(1-\eta), \quad \mu_2 = \frac{\kappa(N+1)}{2} + \frac{\gamma\kappa}{4\gamma_c} + \frac{G}{4}(1+\eta), \qquad \mu_4 = \tfrac{\kappa N}{2} \tag{107}$$

$$\mu_a = \frac{G}{4}(1-\eta) - \frac{\kappa}{2} - \frac{\gamma\kappa}{4\gamma_c}, \quad \mu_b = -\frac{\kappa}{2} - \frac{\gamma\kappa}{4\gamma_c} - \frac{G}{4}(1+\eta), \quad \mu_a + \mu_b = -\kappa - \frac{\gamma\kappa}{2\gamma_c} - \frac{G}{2}\eta \tag{108}$$

$$\mu_{12} = \kappa(N+1) + \frac{\gamma\kappa}{2\gamma_c} + \frac{G}{4}(1+\eta), \quad \mu_{34} = \kappa N + \frac{G}{4}(1-\eta) \tag{109}$$

$$\nu_1 = \kappa M_a, \quad \nu_2 = \kappa M_a + \frac{G}{4}\sqrt{1-\eta^2}, \quad \nu_3 = \kappa M_a + \frac{G}{4}\sqrt{1-\eta^2} \tag{110}$$

$$\nu_{12_+} = \nu_{13_+} = 2\kappa M_a + \frac{G}{4}\sqrt{1-\eta^2}, \quad \nu_{12_-} = \nu_{13_-} = -\frac{G}{4}\sqrt{1-\eta^2} \tag{111}$$

$$\nu_a = C_{0_1}\kappa(2n_{\mathrm{th},1}+1), \quad \nu_b = C_{0_2}\kappa(2n_{\mathrm{th},2}+1) \tag{112}$$

For $\gamma_c = \frac{4g^2}{\kappa}$ being the stimulated emission decay constant due to the atom interacts with the cavity modes. The Single-Photon Optomechanical Cooperativity (C_0)

$$C_{0_1} = \frac{4g_{0_1}^2}{\kappa\gamma_m} \tag{113}$$

$$C_{0_2} = \frac{4g_{0_2}^2}{\kappa\gamma_m} \tag{114}$$

g_{0m} optomechanical coupling strength, κ, cavity decay rate, γ_m mechanical damping rate. We now introduce a variable defined by

$$\rho_{11}^{(0)} = \frac{1-\eta}{2} \tag{115}$$

with $-1 \leq \eta \leq 1$. It then follows, for three-level atoms are initially prepared to be in a coherent superposition of the top and bottom levels, that

$$\rho_{33}^{(0)} = \frac{1+\eta}{2}, \quad \rho_{13}^{(0)} = \frac{\sqrt{1-\eta^2}}{2} \tag{116}$$

where we have taken that $\rho_{13}^{(0)} = \rho_{31}^{*(0)}$.

$$[\hat{a}_i\hat{a}_j^n, F(\hat{a}_j, \hat{a}_i, \hat{a}_j^\dagger)] = n\,\hat{a}_i\hat{a}_j^{n-1}\frac{\partial F}{\partial \hat{a}_j^\dagger}, \quad \left[\hat{a}_i^\dagger\hat{a}_j,\ F\right] = \hat{a}_i^\dagger\frac{\partial F}{\partial \hat{a}_j^\dagger} - \frac{\partial F}{\partial \hat{a}_i}\hat{a}_j, \quad \hat{a}_i\hat{a}_i^\dagger = \hat{a}_i^\dagger\hat{a}_i + 1 \tag{117}$$

$$\hat{a}^n\hat{a}^\dagger = \hat{a}^\dagger\hat{a}^n + n\hat{a}^{n-1}, \quad \hat{a}^2\hat{a}^\dagger = \hat{a}^\dagger\hat{a}^2 + 2\hat{a}, \quad \hat{a}_1^\dagger\hat{a}_1\hat{a}_1^\dagger = \hat{a}_1^\dagger(\hat{a}_1^\dagger\hat{a}_1 + 1) \tag{118}$$

$$[\hat{a}_1, \hat{a}_1\hat{a}_1^\dagger] = \hat{a}_1[\hat{a}_1, \hat{a}_1^\dagger] + [\hat{a}_1, \hat{a}_1]\hat{a}_1^\dagger = \hat{a}_1, \quad \hat{a}_1\hat{a}_1^\dagger\hat{a}_1 = (\hat{a}_1^\dagger\hat{a}_1 + 1)\hat{a}_1 = \hat{a}_1^\dagger\hat{a}_1\hat{a}_1 + \hat{a}_1 \tag{119}$$

References

[1] Singh, S. K., Peng, J.-X., Asjad, M., Mazaheri, M. Entanglement and coherence in a hybrid Laguerre–Gaussian rotating cavity optomechanical system with two-level atoms. Journal of Physics B: Atomic, Molecular and Optical Physics. 2021, 54(21), 215502. https://doi.org/10.1088/1361-6455/abf7a0

[2] Singh, S. K., Asjad, M., Ooi, C. H. R. Tunable optical response in a hybrid quadratic optomechanical system coupled with single semiconductor quantum well. Quantum Information Processing. 2022, 21(2), 47. https://doi.org/10.1007/s11128-021-03336-93

[3] Singh, S. K., Ooi, C. H. R. Quantum correlations of quadratic optomechanical oscillator. Journal of the Optical Society of America B. 2014, 31(10), 2390–2398. https://doi.org/10.1364/JOSAB.31.002390

[4] Singh, S. K., Mazaheri, M., Peng, J.-X., Sohail, A., Gu, Z., Asjad, M. Normal mode splitting and optical squeezing in a linear and quadratic optomechanical system with optical parametric amplifier. Quantum Information Processing. 2023, 22(5), 198. https://doi.org/10.1007/s11128-023-03969-4

[5] Singh, S. K., Mazaheri, M., Peng, J.-X., Sohail, A., Khalid, M., Asjad, M. Enhanced weak force sensing based on atom-based coherent quantum noise cancellation in a hybrid cavity optomechanical system. Frontiers in Physics. 2023, 11, 1142452. https://doi.org/ 10.3389/fphy.2023.1142452

[6] Jia, J., Huang, J., Zhang, F., Zhang, M. Entanglement between microwave fields and squeezing of the optical output field in an opto-magnomechanical ring cavity. Scientific Reports. 2025, 15(1), 11606. https://doi.org/10.1038/s41598-025-11606-x

[7] Kundu, A., Singh, S. K. Heisenberg-Langevin formalism for squeezing dynamics of linear hybrid optomechanical system. International Journal of Theoretical Physics. 2019, 58(8), 2418–2427. https://doi.org/10.1007/s10773-019-04048-5

[8] Singh, S. K., Muniandy, S. V. Temporal dynamics and nonclassical photon statistics of quadratically coupled optomechanical systems. International Journal of Theoretical Physics. 2016, 55(1), 287-301. https://doi.org/10.1007/s10773-015-2828-5

[9] Yusoff, F. N., Zulkifli, M. A., Ali, N., Singh, S. K., Abdullah, N., Ahmad Hambali, N. A. M., Edet, C. O. Tunable transparency and group delay in cavity optomechanical systems with degenerate Fermi gas. Photonics. 2023, 10(3), 279. https://doi.org/ 10.3390/photonics10030279

[10] Bronnikov, K. A. 2nd Comment on "On the Klein–Gordon oscillator in topologically charged Ellis–Bronnikov type wormhole spacetime". The European Physical Journal Plus. 2024, 139(3), 283. https://doi.org/ 10.1140/epjp/s13360-024-05136-8

[11] Amazioug, M., Daoud, M., Singh, S. K., Asjad, M. Strong photon antibunching effect in a double-cavity optomechanical system with intracavity squeezed light. Quantum Information Processing. 2023, 22(8), 301. https://doi.org/10.1007/s11128-023-03964-9

[12] Kharroube, K. A. Moments of Inertia, Magnetic Dipole Moments, and Electric Quadrupole Moments of the Lithium Isotopes. Open Journal of Microphysics. 2023, 13(4), 69-97. https://doi.org/10.4236/ojm.2023.134004

[13] Tanji, K., Takahashi, H., Roga, W., Takeoka, M. Rate-fidelity tradeoff in cavity-based remote entanglement generation. Physical Review A. 2024, 110(4), 042405. https://doi.org/10.1103/PhysRevA.110.042405

[14] Qasymeh, M., Hunza, M., Asjad, M., Abbas, T., Teklu, B., Eleuch, H. Tunable Electromagnetically Induced Multi-Transparencies in Hybrid Optomechanical System Incorporating Atomic Medium. SSRN Electronic Journal. 2022. https://doi.org/ 10.2139/ssrn.4210409

[15] Qasymeh, M., Hunza, M., Asjad, M., Abbas, T., Teklu, B., Eleuch, H. Tunable Electromagnetically Induced Multi-Transparencies in Hybrid Optomechanical System Incorporating Atomic Medium. SSRN Electronic Journal. 2022. https://doi.org/10.2139/ssrn.4210409

[16] Singh, S. K., Peng, J.-X., Asjad, M., Mazaheri, M. Entanglement and coherence in a hybrid Laguerre–Gaussian rotating cavity optomechanical system with two-level atoms. Journal of Physics B: Atomic, Molecular and Optical Physics. 2021, 54(21), 215502. https://doi.org/ 10.1088/1361-6455/abf7a0

[17] Quantum Information Processing. 2022, 21, 47. https://doi.org/10.1007/s11128-022-03424-6

[18] Mari, A., Giovannetti, V., Mancini, S. Quantum state engineering by reservoir engineering. Journal of the Optical Society of America B. 2014, 31(10), 2390. https://doi.org/10.1364/JOSAB.31.002390

[19] Physics Letters A. 2022, 442, 128181. https://doi.org/10.1016/j.physleta.2022.128181

[20] Quantum Information Processing. 2023, 22, 198. https://doi.org/10.1007/s11128-023-03969-4

[21] Chan, J., Alegre, T. P. M., Safavi-Naeini, A. H., Hill, J. T., Krause, A., Gröblacher, S., Aspelmeyer, M., Painter, O. Laser cooling of a nanomechanical oscillator into its quantum ground state. Nature. 2011, 478(7367), 89–92. https://doi.org/10.1038/nature10461

[22] Wang, Y.-D., Clerk, A. A. Reservoir-engineered entanglement in optomechanical systems. Physical Review Letters. 2013, 110(25), 253601. https://doi.org/10.1103/PhysRevLett.110.253601

[23] Ma, Y.-H., Li, F.-Z., Han, X.-G., Wu, E. Generation of Steady-State Entanglement in Quadratically Coupled Optomechanical System Assisted by Two-Level Atoms. International Journal of Theoretical Physics. 2016, 55(5), 2386–2396. https://doi.org/10.1007/s10773-016-2965-6

[24] Ma, Y.-H., Li, F.-Z., Han, X.-G., Wu, E. Generation of Steady-State Entanglement in Quadratically Coupled Optomechanical System Assisted by Two-Level Atoms. International Journal of Theoretical Physics. 2016, 55(5), 2386-2396. https://doi.org/10.1007/s10773-015-2784-7

[25] Fernández-Lorenzo, S., Porras, D. Quantum sensing close to a dissipative phase transition: Symmetry breaking and criticality as metrological resources. Physical Review A. 2017, 96(1), 013817. https://doi.org/10.1103/PhysRevA.96.013817

[26] Fadel, M., Gessner, M. Relating spin squeezing to multipartite entanglement criteria for particles and modes. Physical Review A. 2020, 102(1), 012412. https://doi.org/10.1103/PhysRevA.102.012412

[27] Aspelmeyer, M., Kippenberg, T. J., Marquardt, F. Cavity optomechanics. Reviews of Modern Physics. 2014, 86(4), 1391-1452. https://doi.org/10.1103/revmodphys.86.1391

[28] Hartmann, M. J., Brandão, F. G. S. L., Plenio, M. B. Quantum many-body phenomena in coupled cavity arrays. Laser and Photonics Reviews. 2008, 2(6), 527-556. https://doi.org/10.1002/lpor.200810046

[29] Chan, J., Alegre, T. P. M., Safavi-Naeini, A. H., Hill, J. T., Krause, A., Gröblacher, S., Aspelmeyer, M., Painter, O. Laser cooling of a nanomechanical oscillator into its quantum ground state. Nature. 2011, 478(7367), 89–92. https://doi.org/10.1038/nature10461

[30] Verhagen, E., Deléglise, S., Weis, S., Schliesser, A., Kippenberg, T. J. Quantum-coherent coupling of a mechanical oscillator to an optical cavity mode. Nature. 2012, 482(7383), 63–67. https://doi.org/10.1038/nature10787

[31] Salih, E., Getahun, M. Two-mode light in optomechanical cavity with squeezed vacuum reservoir. Scientific Reports. 2025, 15(1), 4870. https://doi.org/10.1038/s41598-025-88382-w

[32] Genes, C., Mari, A., Vitali, D., Tombesi, P. Quantum effects in optomechanical systems. Advances in Atomic, Molecular, and Optical Physics. 2009, 57, 33-86. https://doi.org/10.1016/S1049-250X(09)57002-3

[33] Wang, Y.-D., Clerk, A. A. Reservoir-engineered entanglement in optomechanical systems. Physical Review Letters. 2013, 110(25), 253601. https://doi.org/10.1103/PhysRevLett.110.253601

[34] Amaro-Seoane, P., Audley, H., Babak, S., Baker, J., Barausse, E., Bender, P., Berti, E., Binetruy, P., Born, M., Bortoluzzi, D., et al. Laser interferometer space antenna. arXiv preprint arXiv: 1702.00786. 2017. https://arxiv.org/abs/1702.00786

[35] Teufel, J. D., Donner, T., Li, D., Harlow, J. W., Allman, M. S., Cicak, K., Sirois, A. J., Whittaker, J. D., Lehnert, K. W., Simmonds, R. W. Sideband cooling of micromechanical motion to the quantum ground state. Nature. 2011, 475(7356), 359–363. https://doi.org/10.1038/nature10261

[36] Treutlein, P., Genes, C., Hammerer, K., Poggio, M., Rabl, P. Hybrid Mechanical Systems. In: Cavity Optomechanics. Springer, Berlin, Heidelberg; 2014, pp. 327-351.